Since January 2020 Elsevier has created a COVID-19 resource centre with free information in English and Mandarin on the novel coronavirus COVID-19. The COVID-19 resource centre is hosted on Elsevier Connect, the company's public news and information website.

Bioorganic & Medicinal Chemistry 21 (2013) 412–424

Contents lists available at SciVerse ScienceDirect

Bioorganic & Medicinal Chemistry

journal homepage: www.elsevier.com/locate/bmc

Design and synthesis of new tripeptide-type SARS-CoV 3CL protease inhibitors containing an electrophilic arylketone moiety

Sho Konno [a,†], Pillaiyar Thanigaimalai [a,†], Takehito Yamamoto [a], Kiyohiko Nakada [a], Rie Kakiuchi [a], Kentaro Takayama [a], Yuri Yamazaki [a], Fumika Yakushiji [a], Kenichi Akaji [b], Yoshiaki Kiso [b], Yuko Kawasaki [c], Shen-En Chen [c], Ernesto Freire [c], Yoshio Hayashi [a,*]

[a] Department of Medicinal Chemistry, Tokyo University of Pharmacy and Life Sciences, Tokyo 192-0392, Japan
[b] Department of Medicinal Chemistry, Kyoto Pharmaceutical University, Kyoto 607-8412, Japan
[c] Department of Biology, Johns Hopkins University, Baltimore, MD, USA

ARTICLE INFO

Article history:
Received 1 October 2012
Revised 10 November 2012
Accepted 12 November 2012
Available online 24 November 2012

Keywords:
Peptidomimetics
SARS-CoV 3CL protease
Cysteine protease inhibitors
Docking study
SARS

ABSTRACT

We describe here the design, synthesis and biological evaluation of a series of molecules toward the development of novel peptidomimetic inhibitors of SARS-CoV 3CL^{pro}. A docking study involving binding between the initial lead compound **1** and the SARS-CoV 3CL^{pro} motivated the replacement of a thiazole with a benzothiazole unit as a warhead moiety at the P1′ site. This modification led to the identification of more potent derivatives, including **2i, 2k**, **2m**, **2o**, and **2p**, with IC_{50} or K_i values in the submicromolar to nanomolar range. In particular, compounds **2i** and **2p** exhibited the most potent inhibitory activities, with K_i values of 4.1 and 3.1 nM, respectively. The peptidomimetic compounds identified through this process are attractive leads for the development of potential therapeutic agents against SARS. The structural requirements of the peptidomimetics with potent inhibitory activities against SARS-CoV 3CL^{pro} may be summarized as follows: (i) the presence of a benzothiazole warhead at the S1′-position; (ii) hydrogen bonding capabilities at the cyclic lactam of the S1-site; (iii) appropriate stereochemistry and hydrophobic moiety size at the S2-site and (iv) a unique folding conformation assumed by the phenoxyacetyl moiety at the S4-site.

1. Introduction

Severe acute respiratory syndrome (SARS), a typical form of pneumonia, was first reported in southern China in November 2002. SARS rapidly spread to 32 countries, creating panic among the public and in the World Health Organization (WHO).[1–3] The initial outbreak of SARS included more than 8000 individuals diagnosed with the disease. Of these, 774 lives were claimed.[4] SARS is characterized by a high fever (>38 °C), malaise, headache, rigor and a non-productive cough.[5] The causative agent of SARS has been identified as a novel human coronavirus (SARS-CoV)[6] that encodes several viral proteases that proteolyze polyproteins to yield functional proteins. One such highly conserved cysteine protease is the main protease (M^{pro}), also known as the dimeric chymotrypsin-like protease (3CL^{pro}).[7–9] 3CL^{pro} mediates the majority of proteolytic processes involved in producing two large viral polyproteins, replicases pb1a and pb1b.[7–9] The active site of SARS-CoV 3CL^{pro} contains Cys145 and His41, which together constitute a catalytic dyad in which the cysteine moiety functions as a common nucleophile in the proteolytic process.[9,10] Since SARS-CoV 3CL^{pro} plays an important role in the virus life cycle, it has been recognized as a key target for the discovery of anti-SARS agents. Numerous SARS-CoV 3CL^{pro} inhibitors have been identified through chemical library screenings[11–16] or rational design approaches based on the active site properties.[17–20] These protease inhibitors include C2-symmetric peptidomimetics,[11] 3-quinolinecarboxylic acid derivatives,[12] bifunctional arylboronic acids,[13] keto-glutamine derivatives,[14] isatin derivatives,[15] thiophene-2-carboxylates,[16] zinc conjugated compounds,[17] cinanserin,[18] calmodulin,[19] benzotriazoles,[20] α,β-unsaturated acids,[21] anilide,[22] and glutamic acid and glutamine peptides possessing a trifluoromethyl ketone group.[23,24]

In our ongoing effort to develop anti-SARS agents, we previously identified a series of *Z*-Val-Leu-Ala(pyrrolidone-3-yl)-2-thiazoles as SARS-CoV 3CL^{pro} inhibitors.[25] Among these compounds, compound **1** (Fig. 1) was identified as a potent lead compound with a K_i value of 2.20 μM.[25]

Primary structure–activity relationship (SAR) studies of **1** have revealed that the presence of a rigid cyclic amide (P1-site) and the electron-withdrawing chemical warhead thiazolyl-2-ketone (P1′-moiety) are very important for the inhibitory activity. In the present study, we performed a molecular modeling study involving **1** and the 3CL^{pro}. The study revealed the presence of a space in the

* Corresponding author. Tel./fax: +81 42 676 3275.
E-mail address: yhayashi@toyaku.ac.jp (Y. Hayashi).
† These authors contributed equally to this work.

0968-0896/$ - see front matter © 2012 Elsevier Ltd. All rights reserved.
http://dx.doi.org/10.1016/j.bmc.2012.11.017

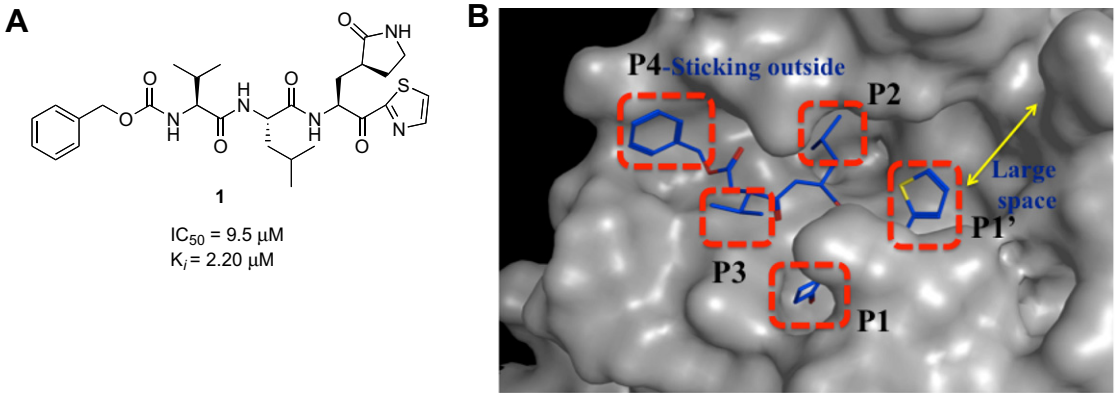

Figure 1. Structure of a lead compound **1** (A) and their molecular stimulated representation (B).

S1′-pocket that was larger than the size of the thiazole unit, and the N-terminal P4-moiety protruded from the binding site (Fig. 1B). Thus, P1′ and P4 were sequentially optimized in a step-by-step approach that involved testing a wide variety of substructural substitutions in **1**. The P2 and P1- sites were focused in parallel. As a result, some analogs were identified that exhibited potent inhibitory activity on the submicromolar to nanomolar range. Here we describe the results of these extensive studies in detail, including the design, synthesis, molecular modeling and biological evaluation of a series of SARS-CoV $3CL^{pro}$ inhibitors.

2. Chemistry

$3CL^{pro}$ inhibitors are generally synthesized by assembling two key fragments: dipeptidic **9** and the C-terminal thiazole derivatives **13** or **17**. The dipeptides **9** were prepared via Fmoc-based solid-phase peptide synthesis over Wang resin. The corresponding Fmoc-amino acids were introduced onto the resin via diisopropylcarbodiimide (DIC)-mediated coupling in the presence of catalytic amounts of 4-*N*,*N*′-dimethylaminopyridine (DMAP) in DMF (Scheme 1). The resulting intermediate **6** was treated with 20% piperidine in DMF to remove the Fmoc- group and coupled to Fmoc-valine, yielding **7**, via the DIC-HOBt (1-hydroxybenzotriazole) method in DMF. Further Fmoc-deprotection and the reaction of **7** with various carboxylic acids or acid chlorides produced the crucial P4-attached dipeptides **9** after treatment of resin **8** with trifluoroacetic acid/water (10:1) for 1 h. The dipeptides **9** were used directly in the next step without further purification.

The syntheses of key intermediates on the path to the thiazoles **13**, as well as the title inhibitors **2**, **3** and **5**, are indicated in Scheme 2. The optically pure glutamic acid ester **10** was converted to γ-lactam-acid **11**[26,27] by treatment with bromoacetonitrile, followed by reduction with PtO_2 (5%), cyclization and hydrolysis. Further coupling of **11** to *N*,*O*-dimethylhydroxylamine via the 1-ethyl-3-(3-dimethylaminopropyl)carbodiimide·hydrochloride (EDC·HCl)-HOBt method yielded the Weinreb amide **12**.[26] The Weinreb amide was then coupled to an appropriate thiazole in the presence of *n*-butyl lithium (*n*-BuLi) or lithium diisopropylamide (LDA) at −78 °C to afford the thiazoles **13**, which were deprotected and subsequently reacted with the dipeptides **9** in the presence of *O*-benzotriazole-*N*,*N*,*N*′,*N*′-tetramethyluroniumhexafluoro phosphate (HBTU), HOBt, and DIPEA in DMF to afford the title compounds **2**, **3** and **5**.

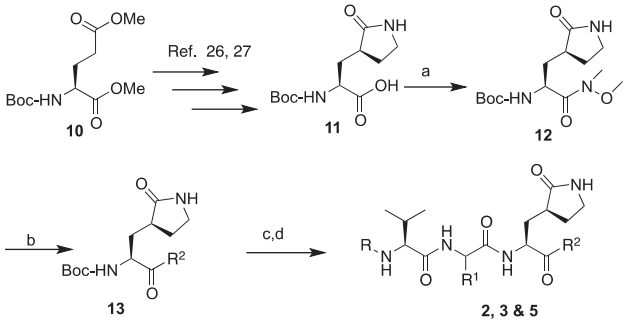

Scheme 2. Synthetic outline for the preparation of title compounds **2**, **3** and **5**. Reagents and conditions: (a) HN(OMe)Me, EDC·HCl, HOBT, Et_3N/DMF; (b) *n*-BuLi, THF, −78 °C (if R^2 = thiazole, 4,5-dimethylthiazole or benzothiazole) or LDA, THF, −78 °C (if R^2 = 5-arylated thiazoles); (c) TFA/H_2O; (d) **9**, HBTU, DIPEA/DMF followed by HPLC purification. Note: The substituents R(acyl), R^1 and R^2 are indicated in Tables 1–3.

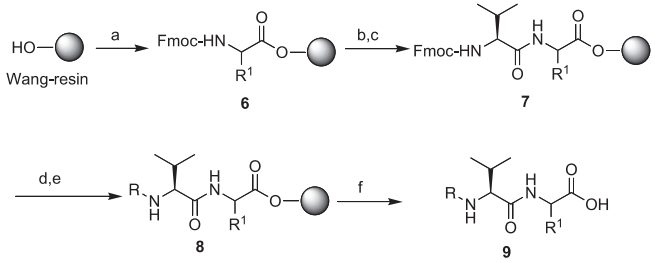

Scheme 1. Solid-phase synthesis of dipeptidic **9**. Reagents and conditions: (a) Fmoc-R^1-OH, DIC, DMAP/DMF; (b) 20% piperidine/DMF; (c) Fmoc-Val-OH, DIC, DMAP, HOBt/DMF; (d) 20% piperidine/DMF; (e) R(Acyl)-Cl, Et_3N or R(Acyl)-OH, DIC, HOBt/DMF; (f) TFA/H_2O. Note: The substituents R (acyl) and R^1 are indicated in Tables 1–3.

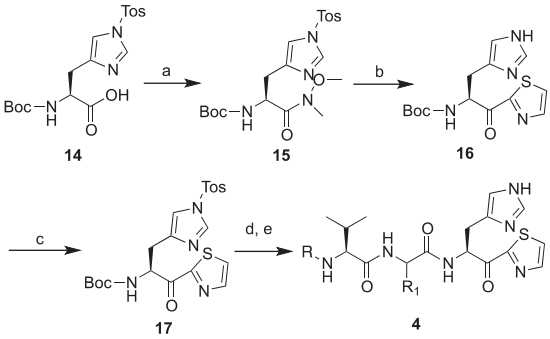

Scheme 3. Synthetic outline for the preparation of imidazole type compounds **4**. Reagents and conditions: (a) HN(OMe)Me, EDC·HCl, HOBT, Et_3N/DMF; (b) thiazole, *n*-BuLi, THF, −78 °C; (c) TsCl, Et_3N, THF; (d) TFA/H_2O; (e) **9**, HBTU, DIPEA/DMF followed by HPLC purification. Note: The substituents R(acyl) and R^1 are indicated in Table 2.

The imidazole-type compounds **4** were prepared as indicated in Scheme 3. Another key imidazole thiazole **17** was prepared from the commercially available Boc-His(Tos)-OH **14** using the same reactions and conditions as indicated for the preparation of the γ-lactam thiazoles **13**. The tosyl-protected **17** was successfully converted to the imidazole-type analogs **4** via deprotection and coupling chemistry, as described for the preparation of **2**, **3** and **5**.

3. Results and discussion

The abilities of the synthetic compounds to inhibit the protease activity of SARS-CoV 3CL^{pro} were evaluated. Briefly, IC_{50} value of each inhibitor was assessed from the apparent decrease of a substrate (H-TSAVLQSGFRK-NH_2) by the digestion with R188I SARS 3CL^{pro} as described previously.[28,29] Cleavage reaction was monitored analytical HPLC and the cleavage rates were calculated from the decrease of the substrate peak area. Determining the kinetic parameters at a constant substrate concentration and different inhibitor concentrations assessed K_i values. The initial rate measurements were determined as previously described using a fluorescence-based peptide cleavage assay with a fluorogenic substrate, Dabcyl-KTSAVLQSGFRKME-Edans.[24,30] The rate of substrate cleavage was detected by the increase in fluorescent over time (see Section 6.7). Tables 1–3 report the IC_{50} and/or K_i values as the mean of 3 independent experiments.

In our previous report, inhibitor **1** was found to be a moderate SARS-CoV 3CL^{pro} inhibitor with an IC_{50} value of 9.5 μM and a K_i value of 2.20 μM. In a first attempt to investigate the effects of the N-terminal substituents (P4-moiety) on the activity profile of **1** (Table 1), the inhibitory activities of a series of aromatic (**2a** & **2b**) and aliphatic (**2c** & **2d**) carbamates were evaluated. None of these compounds showed inhibitory potency comparable to **1**. The same result was obtained for the acyl derivatives, such as **2e** and **2f**. Interestingly, the derivative **2g** (IC_{50} = 6.8 μM), a phenoxymethyl

Table 1
Inhibitory activities of compounds (**2a**–**u**)

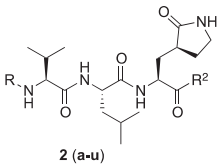

2 (a-u)

Entry no.	R	R^2	Inhibition		Entry no.	R	R^2	Inhibition	
			IC_{50} (μM)	K_i (μM)				IC_{50} (μM)	K_i (μM)
2a	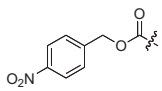		36	NT	**2l**	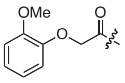		1.9	NT
2b	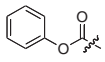		85	NT	**2m**	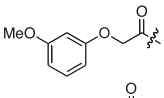		0.75	NT
2c	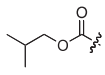		250	NT	**2n**	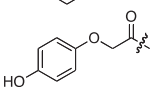		1.2	0.011
2d	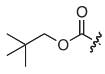		280	NT	**2o**	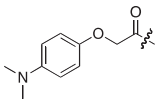		0.65	NT
2e	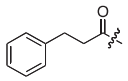		13	NT	**2p**	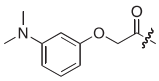		NT	0.003
2f			24	NT	**2q**	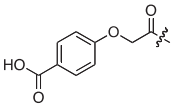		1.7	NT
2g	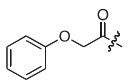		6.8	NT	**2r**	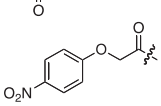		3.4	NT
2h	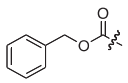		2	NT	**2s**	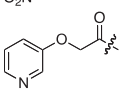		2.9	0.22
2i	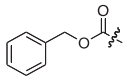		1.7	0.0041	**2t**	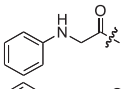		1.5	0.22
2j	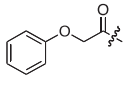		2.3	0.022	**2u**	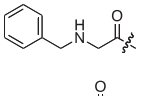		7.5	NT
2k			0.92	0.014	**1**			9.5	NT

NT = not tested.

Table 2
Inhibitory activities of compounds (**3a–d** & **4a–c**)

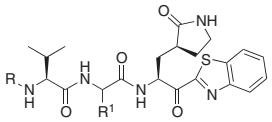

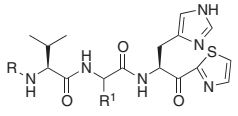

Entry no.	R	R^1	Inhibition IC_{50} (μM)	Entry no.	R	R^1	Inhibition IC_{50} (μM)
3a	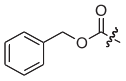		>1600	**4a**	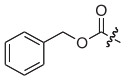		260
3b	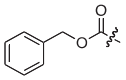		NT	**4b**	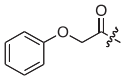		210
3c	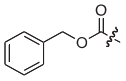		NT	**4c**	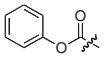		>1600
3d	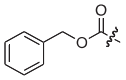		>1600	**1**	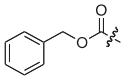		9.5

NT = not tested.

Table 3
Inhibitory activities of compounds (**5a–i**)

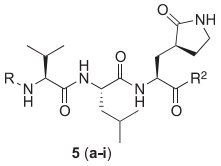

Entry no.	R	R^2	Inhibition K_i (μM)	Entry no.	R	R^2	Inhibition K_i (μM)
5a	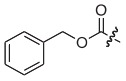	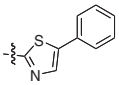	0.06	**5f**	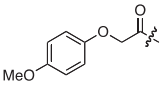	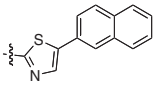	22
5b	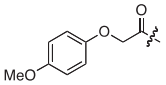	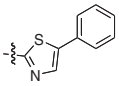	0.27	**5g**	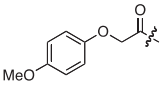	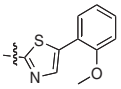	0.47
5c	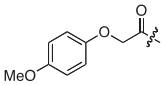	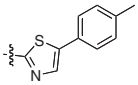	1.46	**5h**	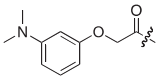	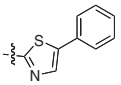	0.17
5d	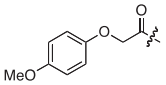	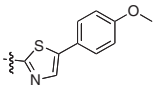	56	**5i**	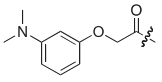		0.33
5e	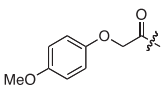	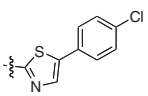	1.3	**2i**	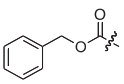		0.0041

carbonyl, displayed a slightly higher activity than **1**. Thus, the presence of the phenoxymethyl carbonyl at the N-terminal position appeared to enhance the activity of **1**.

The molecular modeling study involving **1** and the $3CL^{pro}$ enzyme (Fig. 1) provided insight and understanding into the binding of the inhibitor to the active site of the enzyme (See Section 4 and Fig. 2). The introduction of a spacious warhead group (P1′) was suggested as a means for increasing the inhibitory activity; therefore, we modified inhibitor **1** to include larger units, such as 4,5-dimethylthiazole, 5-methylthiazole, benzothiazole and a series of 5-arylated thiazoles at the P1′ position.

The compound bearing 4,5-dimehtylthiazole, **2h**, displayed a lower inhibitory activity (IC_{50} = 22 μM) than **1**. Compounds **2i** and **2j** bearing benzothiazole exhibited four- to fivefold higher activities (**2i**; IC_{50} = 1.7 μM, **2j**; IC_{50} = 2.3 μM) than **1** and 10- to 13-fold higher activities than **2h**. Notably, **2i** exhibited very potent inhibition with a K_i value of 4.1 nM. This finding strongly suggested that the benzothiazole unit in **1** was a suitable chemical warhead group for occupying the S1′-site. In the subsequent studies, inhibitors **2i** and **2j** were advanced as lead compounds for further optimization.

A series of electron-donating or electron-withdrawing substituents were introduced onto the phenyl ring of the P4-moiety of **2j**. Indeed, compounds with an electron donating substituent such as methoxy, hydroxyl, or *N,N*′-dimethylamino at the *o*-, *p*- or *m*-positions (**2k**, **2l** or **2m**: *p*-, *o*- or *m*-methoxy, respectively;

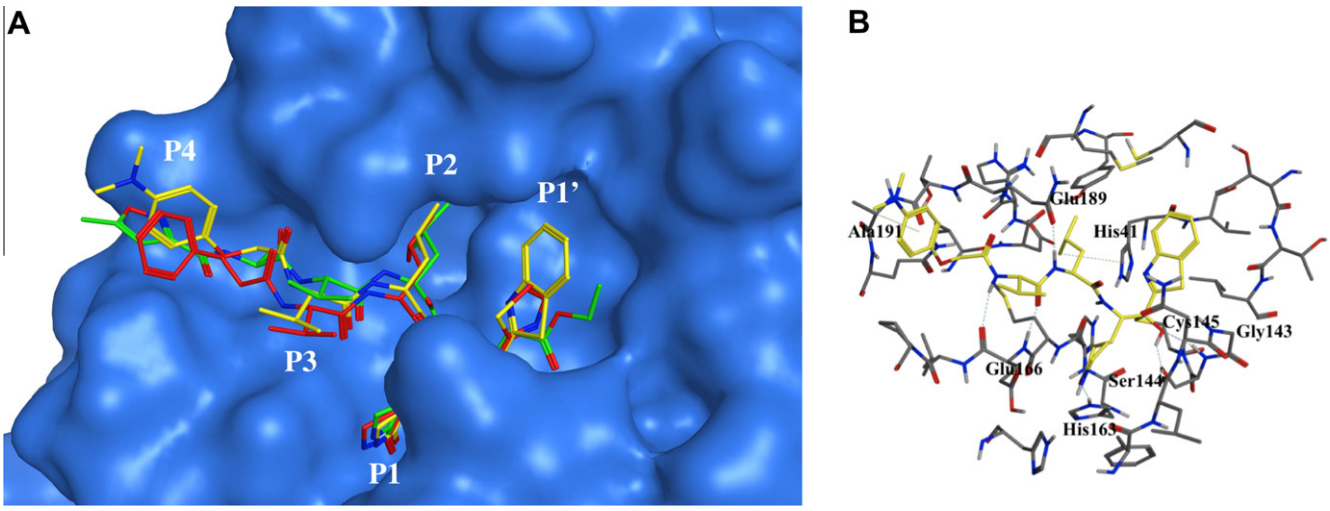

Figure 2. Molecular dynamics stimulated pose of compound **2o**, (yellow stick) bound to SARS-CoV 3CLpro (PDB ID: 1WOF (green stick) with blue molecular surface); with lead compound **1** (red stick); (A) overlapped view of **2o** with an original vinyl ester (green stick) and lead **1** (red stick); (B) contacted residues with hydrogen bonding interactions (dotted lines).

2n: *p*-hydroxyl; and **2o** or **2p**: *p*- or *m*-*N*,*N*′-dimethylamino, respectively) exhibited more potent inhibition than **2j**. The *m*-methoxy (**2m**: IC_{50} = 0.75 μM) and *p*-*N*,*N*′ dimethylamino (**2o**: IC_{50} = 0.65 μM) analogs stood out in their inhibitory strengths. The most promising inhibitor was the *m*-*N*,*N*′-dimethylamino derivative (**2p**), with a K_i value of 3.1 nM; however, analogs with an electron-withdrawing substituent (**2q**: *p*-carboxyl or **2r**: *p*-nitro) displayed relatively low potencies. These results strongly suggested that an electron-donating substituent on the phenyl ring of the P4-moiety was important and favorable to enhance inhibitory activity against $3CL^{pro}$.

Isosteric replacement around the P4-scaffold in the context of **2j** yielded notable differences from the inhibitory activities of **2j**. Replacement of phenoxy (**2j**) with pyridinyloxy (**2s**) did not hamper the inhibitory potency. Interestingly, the potency was recovered upon phenylamino substitution (**2t**: IC_{50} = 1.5 μM). The chain length between the P4-carbonyl and the phenyl group contributed significantly to the inhibitor potency, as indicated by a decreased in the activity of the analog **2u** (IC_{50} = 7.5 μM).

A variety of substituent groups were introduced into the P2-moiety (**3a**–**d**; Table 2). Initially, the stereochemistry of P2 and a size-appropriate amino acid residue at the S2-position in **2i** were tested. Compound **3a**, in which L-leucine was replaced with D-leucine, dramatically reduced the inhibitory activity. Replacement with bulky hydrophobic side chains, such as cyclohexylmethyl (**3b**) and benzyl (**3c**) resulted in solubility issue in the enzyme assay, and replacement with polar glutamic acid (**3d**) did not increase the inhibitory potency. L-leucine, therefore, appeared to provide a suitable stereochemistry and appropriate size for the P2-moiety to fit into the S2-pocket. This result also well correlated with the docking study.

The hydrogen-bonding property of the pyrrolidone structure at the P1-side chain of **1** was studied with an imidazole moiety. As shown in Table 2, none of these compounds (**4a**–**c**) exhibited notable inhibitory activity against SARS-CoV $3CL^{pro}$. Thus, the cyclic amide (γ-lactam) at the P1 site was crucial for potent inhibitory activity.

The P1′-moiety was next examined by varying the 5-substituted thiazoles (**5a**–**i**; Table 3). The inhibitory activities (K_i values) of compounds **5a**–**i** are listed in Table 3. Analog **5a** (K_i = 60 nM) showed 15-times lower activity than **2i**; however, the other 5-arylated thiazoles (**5b**–**i**) generally exhibited very low inhibitory activities compared to **5a**, although the K_i values of some inhibitors, including **5b**, **5g**–**i**, were in the submicromolar range. These studies confirmed that the benzothiazole unit was appropriate as a warhead group for the P1′-moiety.

4. Docking study

Previously, we demonstrated that the inhibitory activity of a compound containing a thiazole residue for insertion into the S1′-pocket was not time-dependent, suggesting a reversible strong binding interaction with the protease.[25,27] Here, we examined the molecular docking of the potent active compound, **2o**, in comparison with the lead compound **1** and a structurally similar ligand,[31] the docking structure of which has been elucidated by x-ray crystallography (PDB ID: 1WOF, K_i = 10.7 μM)[31] (Fig. 2). Several minimization processes were performed using the MMFF94X force field to model the solvation environment surrounding the inhibitor. A molecular simulation was subsequently performed. Figure 2A shows that the **2o** moieties P1–P3 (yellow stick) interacted with the same region of the enzyme as the lead **1**. Interestingly, the benzothiazole unit occupied the S1′-pocket more tightly than the smaller thiazole moiety. The minimized energies for **2o** and **1** obtained from the docking study were −43.65 and −37.56 kcal/mol, respectively.[32] Additionally, the 4-*N*,*N*′-dimethylaminophenoxy acetyl group adopted a unique folding conformation by forming new hydrophobic interactions with α-carbon of Ala 191 at the P4 site, as shown in Figure 2B.

5. Conclusions

We describe here the design, synthesis and biological evaluation of a series of tripeptide-type SARS-CoV $3CL^{pro}$ inhibitors in a SAR study. A docking study of the initial lead compound **1** bound to the SARS-CoV $3CL^{pro}$ provided a better understanding of the inhibitor-active site structure and interactions. These studies led to the development of several potent inhibitors, including **2i**, **2k**, **2m**, **2o**, and **2p** with IC_{50} or K_i values in the submicromolar to nanomolar range. Compounds **2i** and **2p** exhibited the most potent inhibitory activity, with K_i values of 4.1 and 3.1 nM, respectively. These results clearly indicated that the peptidomimetics were promising inhibitors for the development of potential therapeutic agents against SARS. The structural requirements of the peptidomimetics displaying potent inhibitory activity against SARS-CoV $3CL^{pro}$ could be summarized as follows: (i) a benzothiazole unit

was effectively accommodated as a chemical warhead by the S1′-pocket; (ii) hydrogen-bonding capabilities at the cyclic lactam at the S1-position; (iii) appropriate stereochemistry and a size-appropriate L-leucine moiety in the S2-hydrophobic pocket and (iv) a unique folding conformation assumed by the phenoxyacetyl moiety at the S4-site.

6. Experimental

6.1. Materials and methods

Reagents and solvents were purchased from Wako Pure Chemical Ind., Ltd. (Osaka, Japan), and Aldrich Chemical Co. Inc. (Milwaukee, WI) and were used without further purification. Analytical thin-layer chromatography (TLC) was performed on Merck Silica Gel $60F_{254}$ pre-coated plates. Preparative HPLC was performed using a C18 reverse-phase column (19 × 100 mm; SunFire Prep C18 OBD™, 5 μm) with a binary solvent system: a linear gradient of CH_3CN in 0.1% aqueous TFA at a flow rate of 6 mL/min, detected at UV 254 and 222 nm. All solvents used for HPLC were HPLC-grade. All other chemicals were of analytical grade or better. ^1H and ^{13}C NMR spectra were obtained using a JEOL 400 MHz spectrometer, a Varian Mercury 300 spectrometer (300 MHz) or a BRUKER AV600 spectrometer (600 MHz) with tetramethylsilane as an internal standard. High-resolution mass spectra (ESI or EI) were recorded on a micromass Q-Tof Ultima API or a JEOL JMS-GCmate BU-20 spectrometer. Mass spectra (ESI) were recorded on LCMS-2010EV (SHIMADZU).

6.2. General solid-phase synthetic procedure for the preparation of the dipeptides (9)

To the Wang resin (1.0 mmol) in DMF (5 mL) was added Fmoc-amino acid (3 equiv), DIC (3 equiv) and DMAP (0.25 equiv), and the mixture was stirred for 3 h. The resin was filtered, washed with DMF and CH_2Cl_2 and dried under vacuum to yield **6**. After removal of the Fmoc-group using 20% piperidine in DMF over 20 min, the next appropriate amino acid was coupled to the resin using the coupling agents DIC (3 equiv) and HOBt (3 equiv) by solid-phase synthesis techniques. The resulting intermediate **7** was then treated with 20% piperidine in DMF for 20 min to remove the Fmoc-group and subsequently reacted with the corresponding carboxylic acid (3 equiv) by the DIC-HOBt method or acid chloride (3 equiv) in the presence of Et_3N to produce **8**. Finally, the resin was treated with TFA/H_2O (10:1, 2 mL), and the mixture was filtered after 1 h. The filtrate was removed under high vacuum to give the desired dipeptides **9**, which were used directly in the next step without further purification or analysis.

6.2.1. *tert*-Butyl ((*S*)-1-oxo-3-((*S*)-2-oxopyrrolidin-3-yl)-1-(thiazol-2-yl)propan-2-yl)carbamate (13a)[25]

Compound **11** was prepared through sequential reactions from the well-known intermediate **10**, as reported previously.[27]

To a solution of the acid **11** (5.0 g, 12.0 mmol in DMF, 80 mL) was added EDC·HCl (1.85 g, 13.44 mmol), HOBt (1.56 g, 13.44 mmol) and *N,O*-dimethylhydroxylamine (1.31 g, 13.44 mol) at ambient temperature. The solution was cooled to 0 °C and TEA (1.87 mL, 13.44 mmol) was added slowly. After 2 h, the DMF was evaporated and the resulting residue was dissolved in ethyl acetate (100 mL). The organic phase was subsequently washed with 5% citric acid (50 mL), 5% $NaHCO_3$ (50 mL) and brine (50 mL). This organic layer was then dried over Na_2SO_4 and concentrated under reduced pressure to yield the Weinreb amide derivative **12**, which was purified by column chromatography (EtOAc/MeOH = 9.5:0.5).

To a solution of thiazole (1.373 g, 10.0 mmol) in THF at −78 °C was added *n*-BuLi (2.0 mol in THF, 1.67 mL) dropwise over 15 min. After 1 h stirring, the Weinreb amide **12** (0.640 g, 2.0 mmol) in THF was slowly added dropwise over 20 min and the solution was stirred for 3 h. The reaction was quenched with sat. NH_4Cl and allowed to stir at 0 °C for 20 min. The mixture was evaporated and dissolved in ethyl acetate. This solution was washed with water and brine, and then dried over Na_2SO_4. The organic layer was concentrated under reduced pressure and the resulting residue was subjected to flash chromatography (EtOAc/MeOH = 9:1) to obtain the pure compound **13a**.

The data for the compound **12** & **13a** has been reported in a previous article.[25]

Compounds **13b**–**d** were prepared from **12** according to the procedure described for the synthesis of **13a**.

6.2.2. *tert*-Butyl ((*S*)-1-(4,5-dimethylthiazol-2-yl)-1-oxo-3-((*S*)-2-oxopyrrolidin-3-yl)propan-2-yl)carbamate (13b)

51% yield from **12**; yellow solid; ^1H NMR (400 MHz, $CDCl_3$) δ 5.89 (br s, 1H), 5.48–5.46 (m, 1H), 3.40–3.35 (m, 2H), 2.72–2.55, (m, 5H), 2.41 (s, 3H), 2.18–2.00 (m, 3H), 1.44 (s, 9H); HRMS (ESI): *m*/*z* calcd for $C_{17}H_{25}N_3O_4S$ $[M+H]^+$ 367.1566, found 367.1568.

6.2.3. *tert*-Butyl ((*S*)-1-(benzo[*d*]thiazol-2-yl)-1-oxo-3-((*S*)-2-oxopyrrolidin-3-yl)propan-2-yl)carbamate (13c)[25]

Compound **13c**[25] was prepared from **12** using a procedure similar to that described for the preparation of **13a**. The data for the compound **13c** has been reported in a previous article.[25]

6.2.4. *tert*-Butyl ((*S*)-1-(5-methylthiazol-2-yl)-1-oxo-3-((*S*)-2-oxopyrrolidin-3-yl)propan-2-yl)carbamate (13d)[25]

55% yield from **12**; brown solid; ^1H NMR (400 MHz, $CDCl_3$) δ 7.67 (s, 1H), 5.53–5.52 (m, 1H), 3.40–3.38 (m, 2H), 2.65–2.52 (m, 3H), 2.33 (s, 3H), 2.13–1.98 (m, 3H), 1.44 (s, 9H); HRMS (ESI): *m*/*z* calcd for $C_{16}H_{24}N_3O_4S$ $[M+H]^+$ 354.1488, found 354.1491.

6.2.5. *tert*-Butyl ((*S*)-1-oxo-3-((*S*)-2-oxopyrrolidin-3-yl)-1-(5-phenylthiazol-2-yl)propan-2-yl)carbamate (13e)

To a cooled solution of the commercially available 5-phenylthiazole (4.78 mmol) in dry THF at −78 °C, a solution of LDA (6.2 mmol) was slowly added. After 1 h, a pre-cooled solution of Weinreb amide **12** in dry THF was slowly added and the reaction was stirred at −78 °C for 2 h. The solution was allowed to warm to room temperature, was quenched by the addition of water (35 mL), and was extracted with ethyl acetate (3 × 50 mL). The combined organic layers were dried over anhydrous Na_2SO_4, filtered, and evaporated in vacuo. The crude mixture was then purified using flash chromatography (*n*-hexane/EtOAc = 3:7) to furnish **13e**.

55% yield from **12**; brown solid; ^1H NMR (400 MHz, $CDCl_3$) δ 8.16 (s, 1H), 7.63–7.62 (d, J = 8.4 Hz, 2H), 7.47–7.42 (m, 3H), 5.53–5.52 (m, 1H), 3.40–3.38 (m, 2H), 2.65–2.52 (m, 2H), 2.13–1.98 (m, 3H), 1.44 (s, 9H); HRMS (ESI): *m*/*z* calcd for $C_{21}H_{26}N_3O_4S$ $[M+H]^+$ 416.1644, found 416.1653.

Compounds **13f**–**j** were prepared from **12** according to the procedure described for the synthesis of **13e**.

6.2.6. *tert*-Butyl ((*S*)-1-oxo-3-((*S*)-2-oxopyrrolidin-3-yl)-1-(5-(*p*-tolyl)thiazol-2-yl)propan-2-yl)carbamate (13f)

51% yield from **12**; brown solid; ^1H NMR (400 MHz, $CDCl_3$) δ 8.12 (s, 1H), 7.52–7.50 (d, J = 8.0 Hz, 2H), 7.39–7.22 (d, J = 8.0 Hz, 2H), 5.45–5.32 (m, 1H), 3.40–3.26 (m, 2H), 2.65–2.50 (m, 2H), 2.39 (s, 3H), 2.12–1.94 (m, 3H), 1.43 (s, 9H); HRMS (ESI): *m*/*z* calcd for $C_{22}H_{28}N_3O_4S$ $[M+H]^+$ 430.1801, found 430.1802.

6.2.7. *tert*-Butyl ((*S*)-1-(5-(4-methoxyphenyl)thiazol-2-yl)-1-oxo-3-((*S*)-2-oxopyrrolidin-3-yl)propan-2-yl)carbamate (13g)

48% yield from **12**; brown solid; ^{1}H NMR (400 MHz, $CDCl_3$) δ 8.07–8.06 (d, J = 4.0 Hz, 1H), 7.57–7.55 (d, J = 8.8 Hz, 2H), 6.97–6.95 (d, J = 8.4 Hz, 2H), 5.47–53 (m, 1H), 3.81 (s, 3H), 3.39–3.29 (m, 2H), 2.60–2.52 (m, 2H), 2.12–1.93 (m, 3H), 1.44 (s, 9H); HRMS (ESI): m/z calcd for $C_{22}H_{28}N_3O_5S$ $[M+H]^+$ 446.1750, found 446.1754.

6.2.8. *tert*-Butyl ((*S*)-1-(5-(4-chlorophenyl)thiazol-2-yl)-1-oxo-3-((*S*)-2-oxopyrrolidin-3-yl)propan-2-yl)carbamate (13h)

56% yield from **12**; brown solid; ^{1}H NMR (400 MHz, $CDCl_3$) δ 8.14–8.13 (d, J = 4.4 Hz, 1H), 7.56–7.54 (d, J = 8.8 Hz, 2H), 7.44–7.42 (d, J = 8.4 Hz, 2H), 5.51–5.44 (m, 1H), 3.40–3.31(m, 2H), 2.61–2.36 (m, 2H), 2.12–1.93 (m, 3H), 1.44 (s, 9H); HRMS (ESI): m/z calcd for $C_{21}H_{25}ClN_3O_4S$ $[M+H]^+$ 450.1254, found 450.1245.

6.2.9. *tert*-Butyl ((*S*)-1-(5-(naphthalen-2-yl)thiazol-2-yl)-1-oxo-3-((*S*)-2-oxopyrrolidin-3-yl)propan-2-yl)carbamate (13i)

57% yield from **12**; brown solid; ^{1}H NMR (400 MHz, $CDCl_3$) δ 8.29–8.28 (d, J = 4.0 Hz, 1H), 8.11 (s, 1H), 7.92–7.85 (m, 3H), 7.76–7.74 (d, J = 8.4 Hz, 1H), 7.56–7.52 (m, 2H), 5.51–5.43 (m, 1H), 3.41–3.30 (m, 2H), 2.63–2.33 (m, 2H), 2.12–1.91 (m, 3H), 1.45 (s, 9H); HRMS (ESI): m/z calcd for $C_{22}H_{28}N_3O_4S$ $[M+H]^+$ 466.1801, found 466.1798.

6.2.10. *tert*-Butyl ((*S*)-1-(5-(2-methoxyphenyl)thiazol-2-yl)-1-oxo-3-((*S*)-2-oxopyrrolidin-3-yl)propan-2-yl)carbamate (13j)

51% yield from **12**; brown solid; ^{1}H NMR (400 MHz, $CDCl_3$) δ 8.15–8.14 (d, J = 4.0 Hz, 1H), 7.38–7.34 (t, J = 8.0 Hz, 2H), 7.22–7.20 (d, J = 8.0 Hz, 1H), 7.13–7.11 (d, J = 8.0 Hz, 1H), 6.99–6.95 (m, 1H), 5.45–533 (m, 1H), 3.83 (s, 3H), 3.40–3.29 (m, 2H), 2.62–2.33 (m, 2H), 2.10–1.89 (m, 3H), 1.44 (s, 9H); HRMS (ESI): m/z calcd for $C_{22}H_{28}N_3O_5S$ $[M+H]^+$ 446.1750, found 446.1737.

6.2.11. *tert*-Butyl ((2*S*)-3-(4,5-dihydro-1*H*-imidazol-4-yl)-1-(5-methylthiazol-2-yl)-1-oxopropan-2-yl)carbamate (16)

The compound **16** was synthesized from **14** using a method similar to that described for the preparation of **13a**.

51% yield from **14**; brown solid; ^{1}H NMR (300 MHz, $CDCl_3$) δ 8.04 (d, J = 2.93 Hz, 1H), 7.71 (d, J = 2.90 Hz, 1H), 7.58 (s, 1H), 6.74 (s, 1H), 5.64 (br s, 1H), 3.32 (br s, 1H), 1.43 (s, 9H). HRMS (ESI): m/z calcd for $C_{14}H_{18}N_4O_3S$ $[M+H]^+$ 323.1178, found 323.1183.

6.2.12. (*S*)-2,2-Dimethyl-1-(((1-oxo-1-(thiazol-2-yl)-3-(1-tosyl-1*H*-imidazol-4-yl)propan-2-yl)amino)oxy)propan-1-one (17)

To a solution of **16** (1.6 mmol) in THF (20 mL) at 0 °C was added tosyl chloride (1.5 equiv). After 10 min, Et_3N (1.5 equiv) was added slowly and allowed to stir for 3 h at the same condition. The solvent was evaporated and the resulting residue was dissolved in ethyl acetate (50 mL). This organic phase was washed with 5% citric acid (25 mL), 5% $NaHCO_3$ (25 mL) and brine (25 mL). This layer was then dried over Na_2SO_4 and concentrated under reduced pressure to yield **17**, which was purified by column chromatography (*n*-hexane/EtOAc = 5:5).

72% yield from **16**; yellow solid; ^{1}H NMR (300 MHz, $CDCl_3$) δ 8.02 (d, J = 3.2 Hz, 1H), 7.71 (d, J = 2.90 Hz, 1H), 7.60–7.57 (m, 3H), 7.43 (s, 1H), 7.33–7.31 (d, J = 8.1 Hz, 2H), 5.57 (br s, 1H), 2.37 (s, 3H), 1.44 (s, 9H). HRMS (ESI): m/z calcd for $C_{21}H_{24}N_4O_5S_2$ $[M+H]^+$ 477.1300, found 177.1312.

6.3. Synthetic procedure for the preparation of 2a

To a solution of **13a** (2 mmol) in CH_2Cl_2 (2 mL) at 0 °C was added TFA/H_2O (10 mL) and the solution was stirred for 1 h. After evaporating the solvent under reduced pressure, the corresponding deprotected lactam residue (3 mmol) was coupled to the dipeptidic **9** (1.1 equiv) using the coupling agent HBTU (1.1 equiv) and HOBt (1.1 equiv) in the presence of diisopropylethylamine (DIPEA, 1.1 equiv) in DMF (3 mL) at 0 °C. The reaction mixture was allowed to stir for 2–3 h under ambient conditions. The solvent was then evaporated under high vacuum, and the residue was dissolved in ethyl acetate (50 mL). The organic layer was washed with 5% citric acid (25 mL), 5% $NaHCO_3$ (25 mL) and brine (25 mL). This solution was dried over Na_2SO_4, filtered and evaporated under reduced pressure to give a compound **2a**.

Compounds **2f**–**u** were prepared from **13a**–**c** with **9** using a procedure similar to that described for the synthesis of **2a**. Compounds **2a**–**u** were purified by reverse phase HPLC.

6.3.1. 4-Nitrobenzyl ((*S*)-3-methyl-1-(((*S*)-4-methyl-1-oxo-1-(((*S*)-1-oxo-3-((*S*)-2-oxopyrrolidin-3-yl)-1-(thiazol-2-yl)propan-2-yl)amino)pentan-2-yl)amino)-1-oxobutan-2-yl)carbamate (2a)

25% yield from **13a**; white powder; ^{1}H NMR (500 MHz, DMSO-d_6) δ 8.63 (d, J = 7.6 Hz, 1H), 8.26 (d, J = 3.1 Hz, 1H), 8.22 (d, J = 8.6 Hz, 2H), 8.18 (d, J = 3.1 Hz, 1H), 7.93 (d, J = 8.0 Hz, 1H), 7.65 (s, 1H), 7.62 (d, J = 8.6 Hz, 2H), 7.44 (d, J = 8.9 Hz, 1H), 5.46–5.39 (m, 1H), 5.18 (s, 2H), 4.38 (dd, J = 8.4, 14.8 Hz, 1H), 3.88 (dd, J = 7.0, 8.6 Hz, 1H), 3.18 (dd, J = 8.7, 8.8 Hz, 1H), 3.11 (dd, J = 9.2, 16.3 Hz, 1H), 2.48–2.40 (m, 1H), 2.23–2.12 (m, 1H), 2.08–2.01 (m, 1H), 2.00–1.92 (m, 1H), 1.81–1.70 (m, 2H), 1.62–1.53 (m, 1H), 1.48–1.39 (m, 2H), 0.92–0.79 (m, 12H); ^{13}C NMR (125 MHz, DMSO-d_6) δ 191.3, 177.9, 172.2, 170.8, 164.4, 155.8, 146.9, 145.3, 145.2, 128.4, 127.9, 123.4, 64.1, 60.1, 53.0, 50.7, 40.8, 39.4, 37.8, 32.3, 30.4, 27.2, 24.0, 22.9, 21.7, 19.1, 18.1; HRMS (ESI): m/z calcd for $C_{29}H_{39}N_6O_8S$ $[M+H]^+$ 631.2550, found 631.2551.

6.3.2. Phenyl ((*S*)-3-methyl-1-(((*S*)-4-methyl-1-oxo-1-(((*S*)-1-oxo-3-((*S*)-2-oxopyrrolidin-3-yl)-1-(thiazol-2-yl)propan-2-yl)amino)pentan-2-yl)amino)-1-oxobutan-2-yl)carbamate (2b)

26% yield from **13a**; white powder; ^{1}H NMR (500 MHz, DMSO-d_6) δ 8.66 (d, J = 7.6 Hz, 1H), 8.25 (d, J = 3.2 Hz, 1H), 8.17 (d, J = 3.2 Hz, 1H), 7.95 (d, J = 7.9 Hz, 1H), 7.76 (d, J = 8.9 Hz, 1H), 7.64 (s, 1H), 7.36 (t, J = 8.1 Hz, 2H), 7.19 (d, J = 7.5 Hz, 1H), 7.06 (d, J = 7.6 Hz, 2H), 5.46–5.38 (m, 1H), 4.40 (dd, J = 9.0, 15.5 Hz, 1H), 3.89 (dd, J = 7.3, 8.5 Hz, 1H), 3.16 (dd, J = 9.7, 8.5 Hz, 1H), 3.09 (dd, J = 9.1, 16.4 Hz, 1H), 2.48–2.41 (m, 1H), 2.22–2.12 (m, 1H), 2.08–1.93 (m, 2H), 1.81–1.69 (m, 2H), 1.68–1.54 (m, 1H), 1.48–1.35 (m, 2H), 0.93–0.80 (m, 12H); ^{13}C NMR (125 MHz, DMSO-d_6) δ 191.3, 177.9, 172.2, 170.6164.4, 154.3, 151.1, 145.3, 129.2, 128.4, 124.9, 121.6, 60.2, 53.0, 50.8, 40.8, 39.4, 37.8, 32.3, 30.3, 27.2, 24.0, 22.8, 21.8, 19.1, 18.2; HRMS (ESI): m/z calcd for $C_{28}H_{38}N_5O_6S$ $[M+H]^+$ 572.2543, found 572.2531.

6.3.3. Isobutyl ((*S*)-3-methyl-1-(((*S*)-4-methyl-1-oxo-1-(((*S*)-1-oxo-3-((*S*)-2-oxopyrrolidin-3-yl)-1-(thiazol-2-yl)propan-2-yl)amino)pentan-2-yl)amino)-1-oxobutan-2-yl)carbamate (2c)

38% yield from **13a**; white powder; ^{1}H NMR (500 MHz, DMSO-d_6) δ 8.74 (d, J = 8.0 Hz, 1H), 8.12 (d, J = 7.5 Hz, 1H), 8.10 (d, J = 3.2 Hz, 1H), 8.03 (d, J = 3.2 Hz, 1H), 7.94 (d, J = 8.2 Hz, 1H), 5.46–5.39 (m, 1H), 5.18 (s, 2H), 4.38 (dd, J = 8.4, 14.8 Hz, 1H), 3.88 (dd, J = 7.0, 8.6 Hz, 1H), 3.18 (dd, J = 8.7, 8.8 Hz, 1H), 3.11 (dd, J = 9.2, 16.3 Hz, 1H), 2.48–2.40 (m, 1H), 2.23–2.12 (m, 2H), 2.08–2.01 (m, 1H), 2.00–1.92 (m, 1H), 1.81–1.70 (m, 2H), 1.62–1.53 (m, 1H), 1.48–1.39 (m, 2H), 0.92–0.86 (m, 12H), 0.85–0.80 (m, 6H); ^{13}C NMR (125 MHz, DMSO-d_6) δ 191.4, 173.9, 170.2, 169.0, 165.3, 157.1, 144.7, 128.1, 72.5, 60.9, 54.2, 51.6, 40.3, 39.4, 39.8, 33.2, 31.7, 31.0, 27.1, 25.9, 24.2, 23.1, 22.0, 19.1; HRMS (ESI): m/z calcd for $C_{26}H_{41}N_5O_6S$ $[M+H]^+$ 551.2778, found 551.2780.

6.3.4. Neopentyl ((*S*)-3-methyl-1-(((*S*)-4-methyl-1-oxo-1-(((*S*)-1-oxo-3-((*S*)-2-oxopyrrolidin-3-yl)-1-(thiazol-2-yl)propan-2-yl)amino)pentan-2-yl)amino)-1-oxobutan-2-yl)carbamate (2d)

78% yield from **13a**; white powder; ^{1}H NMR (500 MHz, DMSO-d_6) δ 8.61 (d, J = 7.3 Hz, 1H), 8.25 (d, J = 3.1 Hz, 1H), 8.17 (d, J = 3.0 Hz, 1H), 7.87 (d, J = 7.9 Hz, 1H), 7.64 (s, 1H), 7.01 (d, J = 8.9 Hz, 1H), 5.43–5.37 (m, 1H), 4.37 (dd, J = 8.0, 15.3 Hz, 1H), 3.83 (dd, J = 7.0, 8.8 Hz, 1H), 3.70–3.57 (m, 2H), 3.18 (dd, J = 9.4, 9.4 Hz, 1H), 3.09 (dd, J = 9.2, 16.4 Hz, 1H), 2.48–2.39 (m, 1H), 2.22–2.10 (m, 1H), 2.06–1.99 (m, 1H), 1.97–1.84 (m, 1H), 1.80–1.67 (m, 2H), 1.62–1.51 (m, 1H), 1.47–1.33 (m, 2H), 0.93–0.78 (m, 21H); ^{13}C NMR (125 MHz, DMSO-d_6) δ 191.2, 177.9, 172.2, 171.0, 164.4, 156.4, 145.2, 128.4, 72.8, 59.9, 53.0, 50.7, 40.9, 39.4, 37.8, 32.3, 31.4, 30.4, 27.2, 26.2, 24.0, 22.9, 21.7, 19.1, 18.2; HRMS (ESI): m/z calcd for $C_{27}H_{44}N_5O_6S$ [M+H]$^+$ 566.3012, found 566.3008.

6.3.5. (*S*)-4-Methyl-2-((*S*)-3-methyl-2-(3-phenylpropanamido)-butanamido)-*N*-((*S*)-1-oxo-3-((*S*)-2-oxopyrrolidin-3-yl)-1-(thiazol-2-yl)propan-2-yl)pentanamide (2e)

42% yield from **13a**; white powder; ^{1}H NMR (500 MHz, DMSO-d_6) δ 8.57 (d, J = 7.5 Hz, 1H), 8.25 (d, J = 2.9 Hz, 1H), 8.17 (d, J = 2.9 Hz, 1H), 7.92 (d, J = 7.9 Hz, 1H), 7.83 (d, J = 8.9 Hz, 1H), 7.63 (s, 1H), 7.26–7.09 (m, 1H), 5.46–5.38 (m, 1H), 4.32 (dd, J = 8.8, 15.8 Hz, 1H), 4.16 (dd, J = 7.2, 8.7 Hz, 1H), 3.18 (dd, J = 9.2, 8.9 Hz, 1H), 3.08 (dd, J = 9.2, 16.4 Hz, 1H), 2.78 (t, J = 7.6 Hz, 2H), 2.55–2.37 (m, 3H, overlapping with DMSO-d_6), 2.26–2.12 (m, 1H), 2.07–1.99 (m, 1H), 1.93–1.85 (m, 1H), 1.80–1.68 (m, 2H), 1.62–1.52 (m, 1H), 1.47–1.36 (m, 2H), 0.85 (dd, J = 6.5, 26.4 Hz, 6H), 0.76 (dd, J = 6.8, 12.7 Hz, 6H); ^{13}C NMR (125 MHz, DMSO-d_6) δ 191.3, 178.0, 172.2, 171.3, 170.9, 164.4, 145.3, 141.3, 128.4, 128.2, 125.8, 57.4, 53.0, 50.8, 40.7, 39.4, 37.8, 36.6, 32.4, 31.2, 30.6, 27.6, 24.1, 22.9, 21.8, 19.1, 18.1; HRMS (ESI): m/z calcd for $C_{30}H_{42}N_5O_5S$ [M+H]$^+$ 584.2907, found 584.2913.

6.3.6. (*S*)-2-((*S*)-2-Acetamido-3-methylbutanamido)-4-methyl-*N*-((*S*)-1-oxo-3-((*S*)-2-oxopyrrolidin-3-yl)-1-(thiazol-2-yl)propan-2-yl)pentanamide (2f)

37% yield from **13a**; white powder; ^{1}H NMR (500 MHz, CD_3OD) δ 8.74 (d, J = 8.0 Hz, 1H), 8.12 (d, J = 7.5 Hz, 1H), 8.10 (d, J = 3.2 Hz, 1H), 8.02 (d, J = 3.2 Hz, 1H), 7.96 (d, J = 8.2 Hz, 1H), 5.68–5.60 (m, 1H), 4.44 (dd, J = 7.1, 15.5 Hz, 1H), 4.19–4.15 (m, 1H), 3.38–3.30 (m, 2H, overlapping with MeOH), 2.72–2.63 (m, 1H), 2.45–2.37 (m, 1H), 2.18–2.09 (m, 1H), 2.08–2.00 (m, 2H), 1.99–1.96 (s, 3H), 1.74–1.65 (m, 1H), 1.63–1.54 (m, 1H), 0.99–0.90 (m, 12H); ^{13}C NMR (125 MHz, CD_3OD) δ 192.0, 181.8, 174.9, 173.84, 173.7, 173.4, 165.9, 146.3, 128.6, 119.2, 60.3, 60.2, 55.1, 55.0, 53.3, 53.2, 41.9, 41.9, 41.5, 40.0, 34.1, 31.9, 28.7, 25.8, 23.3, 22.4, 22.2, 19.8, 18.7; HRMS (ESI): m/z calcd for $C_{23}H_{36}N_5O_5S$ [M+H]$^+$ 494.2437, found 494.2424.

6.3.7. (*S*)-4-Methyl-2-((*S*)-3-methyl-2-(2-phenoxyacetamido)-butanamido)-*N*-((*S*)-1-oxo-3-((*S*)-2-oxopyrrolidin-3-yl)-1-(thiazol-2-yl)propan-2-yl)pentanamide (2g)

53% yield from **13a**; white powder; ^{1}H NMR (500 MHz, DMSO) δ 8.64 (d, J = 7.7 Hz, 1H), 8.25 (d, J = 2.8 Hz, 1H), 8.17 (d, J = 2.8 Hz, 1H), 8.10 (d, J = 7.8 Hz, 1H), 7.81 (d, J = 9.0 Hz, 1H), 7.64 (br s, 1H), 7.30–7.23 (m, 2H), 6.97–6.90 (m, 5H), 5.45–5.39 (m, 1H), 4.55 (dd, J = 14.7, 19.3 Hz, 2H), 4.35 (dd, J = 8.5, 14.9 Hz, 1H), 4.26 (dd, J = 6.5, 9.0 Hz, 1H), 3.18 (dd, J = 9.5, 8.9 Hz, 1H), 3.09 (dd, J = 9.2, 16.4 Hz, 1H), 2.46–2.41 (m, 1H, overlapping with DMSO), 2.22–2.13 (m, 1H), 2.08–1.92 (m, 2H), 1.60–1.51 (m, 1H), 1.48–1.36 (m, 2H), 0.85 (dd, J = 6.6, 25.7 Hz, 6H), 0.78 (dd, J = 6.5, 26.6 Hz, 6H); ^{13}C NMR (125 MHz, DMSO) δ 191.3, 178.0, 172.1, 172.0, 170.3, 167.4, 157.7, 145.3, 129.5, 128.4, 121.1, 114.6, 66.6, 56.8, 53.0, 52.9, 50.8, 40.7, 39.4, 37.8, 32.3, 31.0, 27.3, 24.1, 22.8, 21.8, 19.1, 17.8; HRMS (ESI): m/z calcd for $C_{29}H_{40}N_5O_6S$ [M+H]$^+$ 586.2699, found 586.2695.

6.3.8. Benzyl ((*S*)-1-(((*S*)-1-(((*S*)-1-(4,5-dimethylthiazol-2-yl)-1-oxo-3-((*S*)-2-oxopyrrolidin-3-yl)propan-2-yl)amino)-4-methyl-1-oxopentan-2-yl)amino)-3-methyl-1-oxobutan-2-yl)carbamate (2h)

47% yield from **13b**; white powder; ^{1}H NMR (500 MHz, CD_3OD) δ 8.09 (d, J = 7.5 Hz, 1H), 7.38–7.26 (m, 5H), 5.60–5.55 (m, 1H), 5.09 (s, 2H), 4.49–4.43 (m, 1H), 3.95 (d, J = 7.1 Hz, 1H), 3.36–3.25 (m, 2H, overlapping with MeOH), 2.68–2.59 (m, 1H), 2.47 (s, 1H), 2.40 (s, 1H), 2.39–2.33 (m, 1H), 2.15- 2.01 (m, 1H), 2.00–1.92 (m, 2H), 1.73–1.64 (m, 1H), 1.62–1.54 (m, 2H), 0.98–0.88 (m, 12H); ^{13}C NMR (125 MHz, CD_3OD) δ 191.7, 181.8, 174.7, 174.2, 160.4, 158.6, 153.3, 138.6, 129.5, 129.0, 128.8, 67.7, 62.0, 54.5, 53.2, 41.9, 41.5, 40.0, 34.3, 32.0, 28.7, 25.8, 23.3, 22.2, 19.8, 18.6, 14.9, 11.9; HRMS (ESI): m/z calcd for $C_{31}H_{44}N_5O_6S$ [M+H]$^+$ 614.3012, found 614.2993.

6.3.9. Benzyl ((*S*)-1-(((*S*)-1-(((*S*)-1-(benzo[*d*]thiazol-2-yl)-1-oxo-3-((*S*)-2-oxopyrrolidin-3-yl)propan-2-yl)amino)-4-methyl-1-oxopentan-2-yl)amino)-3-methyl-1-oxobutan-2-yl)carbamate (2i)

24% yield from **13c**; white powder; ^{1}H NMR (500 MHz, CD_3OD) δ 8.21 (d, J = 8.4 Hz, 1H), 8.11 (d, J = 7.7 Hz, 1H), 7.66–7.57 (m, 2H), 7.37–7.26 (m, 5H), 5.72 (d, J = 8.3 Hz, 1H), 5.09 (s, 2H), 4.52–4.42 (m, 1H), 3.97–3.92 (m, 1H), 3.39–3.32 (m, 2H, overlapping with MeOH), 2.76–2.67 (m, 1H), 2.48–2.37 (m, 1H), 2.26–2.18 (m, 1H), 2.11–1.99 (m, 3H), 1.71–1.53 (m, 3H), 0.99–0.85 (m, 12H); ^{13}C NMR (125 MHz, CD_3OD) δ 193.5, 181.8, 174.9, 174.2, 165.5, 158.6, 154.8, 138.4, 138.2, 129.5, 129.3, 129.0, 128.8, 128.5, 126.5, 123.7, 67.7, 62.0, 55.2, 53.2, 41.9, 41.5, 40.0, 33.8, 32.0, 28.8, 25.8, 23.2, 22.2, 19.8, 18.6; HRMS (ESI): m/z calcd for $C_{33}H_{42}N_5O_6S$ [M+H]$^+$ 636.2856, found 636.2843.

6.3.10. (*S*)-*N*-((*S*)-1-(Benzo[d]thiazol-2-yl)-1-oxo-3-((*S*)-2-oxopyrrolidin-3-yl)propan-2-yl)-4-methyl-2-((*S*)-3-methyl-2-(2-phenoxyacetamido)butanamido)pentanamide (2j)

28% yield from **13c**; white powder; ^{1}H NMR (500 MHz, CD_3OD) δ 8.31 (d, J = 7.2 Hz, 1H), 8.21 (d, J = 7.6 Hz, 1H), 8.11 (d, J = 7.5 Hz, 1H), 7.79 (d, J = 8.7 Hz, 1H), 7.66–7.55 (m, 2H), 7.30 (t, J = 6.5 Hz, 1H), 7.01–6.95 (m, 3H), 5.73 (dd, J = 3.3, 11.6 Hz, 1H), 4.58 (s, 2H), 4.44 (dd, J = 7.0, 15.7 Hz, 1H), 4.33 (dd, J = 7.2, 8.7 Hz, 1H), 3.41–3.30 (m, 2H, overlapping with MeOH), 2.78–2.70 (m, 1H), 2.45–2.41 (m, 1H), 2.25–2.18 (m, 1H), 2.11–2.01 (m, 3H), 1.69–1.53 (m, 3H), 0.98–0.83 (m, 12H); ^{13}C NMR (125 MHz, CD_3OD) δ 193.5, 181.8, 174.8, 173.3, 171.1, 165.5, 159.1, 154.8, 138.4, 130.7, 129.3, 128.5, 126.5, 123.7, 122.9, 115.9, 68.1, 59.4, 55.2, 53.4, 41.8, 41.5, 40.0, 33.8, 32.5, 28.8, 25.8, 23.2, 22.2, 19.8, 18.5; HRMS (ESI): m/z calcd for $C_{33}H_{42}N_5O_6S$ [M+H]$^+$ 636.2856, found 636.2842.

6.3.11. (*S*)-*N*-((*S*)-1-(Benzo[d]thiazol-2-yl)-1-oxo-3-((*S*)-2-oxopyrrolidin-3-yl)propan-2-yl)-2-((*S*)-2-(2-(4-methoxyphenoxy)acetamido)-3-methylbutanamido)-4-methylpentanamide (2k)

11% yield from **13c**; white powder; ^{1}H NMR (500 MHz, CD_3OD) δ 8.21 (d, J = 7.4 Hz, 1H), 8.11 (d, J = 6.9 Hz, 1H), 7.67–7.56 (m, 2H), 6.92 (d, J = 9.2 Hz, 2H), 6.85 (d, J = 9.2 Hz, 2H), 5.73 (dd, J = 3.3, 11.6 Hz, 1H), 4.52 (s, 2H), 4.44 (dd, J = 6.4, 8.8 Hz, 1H), 4.32 (d, J = 7.2 Hz, 1H), 3.74 (s, 3H), 3.39–3.30 (m, 2H, overlapping with MeOH), 2.78–2.69 (m, 1H), 2.48–2.42 (m, 1H), 2.25–2.18 (m, 1H), 2.12–2.01 (m, 3H), 1.68–1.53 (m, 3H), 0.99–0.83 (m, 12H); ^{13}C NMR (125 MHz, CD_3OD) δ 193.5, 181.8, 174.8, 173.2, 171.2, 165.5, 156.3, 154.8, 153.2, 138.4, 129.3, 128.5, 126.5, 123.7,

117.0, 115.8, 69.0, 59.3, 56.1, 55.2, 53.4, 41.8, 41.5, 40.0, 33.8, 32.5, 28.8, 25.8, 23.2, 22.2, 19.8, 18.5; HRMS (ESI): *m*/*z* calcd for $C_{34}H_{44}N_5O_7S$ $[M+H]^+$ 666.2961, found 666.2993.

6.3.12. (*S*)-*N*-((*S*)-1-(Benzo[*d*]thiazol-2-yl)-1-oxo-3-((*S*)-2-oxopyrrolidin-3-yl)propan-2-yl)-2-((*S*)-2-(2-(2-methoxyphenoxy)acetamido)-3-methylbutanamido)-4-methylpentanamide (2l)

18% yield from **13c**; white powder; ^{1}H NMR (500 MHz, CD_3OD) δ 8.29 (d, *J* = 7.2 Hz, 1H), 8.21 (d, *J* = 7.4 Hz, 1H), 8.11 (d, *J* = 8.0 Hz, 1H), 7.99 (d, *J* = 8.5 Hz, 1H), 7.67–7.57 (m, 2H), 7.02 (d, *J* = 7.2 Hz, 3H), 6.92–6.86 (m, 1H), 5.78–5.70 (m, 1H), 4.57 (d, *J* = 3.5 Hz, 2H), 4.44 (dd, *J* = 6.5, 14.1 Hz, 1H), 4.34 (dd, *J* = 7.1, 8.6 Hz, 1H), 3.88 (s, 3H), 3.41–3.32 (m, 2H, overlapping with MeOH), 2.79–2.69 (m, 1H), 2.48–2.41 (m, 1H), 2.26–2.17 (m, 1H), 2.15–1.99 (m, 3H), 1.72–1.53 (m, 3H), 1.00–0.82 (m, 12H); ^{13}C NMR (125 MHz, CD_3OD) δ 193.5, 181.8, 174.9, 173.2, 171.5, 165.5, 154.8, 151.5, 148.9, 138.4, 129.3, 128.5, 126.5, 124.5, 123.7, 122.2, 117.5, 113.6, 70.8, 59.3, 56.5, 55.1, 53.4, 41.8, 41.5, 40.0, 33.9, 32.6, 28.8, 25.8, 23.2, 22.2, 19.7, 18.4; HRMS (ESI): *m*/*z* calcd for $C_{34}H_{43}N_5O_7S$ $[M+H]^+$ 665.2883, found 665.2881.

6.3.13. (*S*)-*N*-((*S*)-1-(Benzo[*d*]thiazol-2-yl)-1-oxo-3-((*S*)-2-oxopyrrolidin-3-yl)propan-2-yl)-2-((*S*)-2-(2-(3-methoxyphenoxy)acetamido)-3-methylbutanamido)-4-methylpentanamide (2m)

14% yield from **13c**; white powder; ^{1}H NMR (500 MHz, CD_3OD) δ 8.22 (d, *J* = 7.4 Hz, 1H), 8.13 (d, *J* = 6.9 Hz, 1H), 7.65–7.54 (m, 2H), 7.06 (d, *J* = 9.2 Hz, 1H), 6.87 (d, *J* = 9.2 Hz, 2H), 6.73 (s, 1H), 5.71 (dd, *J* = 3.3, 11.2 Hz, 1H), 4.54 (s, 2H), 4.41 (dd, *J* = 6.2, 8.8 Hz, 1H), 4.31 (d, *J* = 7.0 Hz, 1H), 3.71 (s, 3H), 3.36–3.27 (m, 2H), 2.77–2.68 (m, 1H), 2.51–2.44 (m, 1H), 2.25–2.18 (m, 1H), 2.13–2.03 (m, 3H), 1.71–1.56 (m, 3H), 0.98 - 0.85 (m, 12H); ^{13}C NMR (125 MHz, CD_3OD) δ 193.5, 181.8, 174.8, 173.2, 171.2, 165.5, 162.5, 160.3, 154.8, 138.4, 131.2, 129.3, 128.5, 126.5, 123.7, 108.7, 107.8, 102.4, 68.2, 59.3, 55.8, 55.2, 53.3, 41.5, 40.0, 33.8, 32.5, 23.2, 22.2, 19.8, 18.5; HRMS (ESI): *m*/*z* calcd for $C_{34}H_{43}N_5O_7S$ $[M+H]^+$ 665.2883, found 665.2882.

6.3.14. (*S*)-*N*-((*S*)-1-(Benzo[*d*]thiazol-2-yl)-1-oxo-3-((*S*)-2-oxopyrrolidin-3-yl)propan-2-yl)-2-((*S*)-2-(2-(4-hydroxyphenoxy)acetamido)-3-methylbutanamido)-4-methylpentanamide (2n)

21% yield from **13c**; white powder; ^{1}H NMR (500 MHz, CD_3OD) δ 8.21 (d, *J* = 8.1 Hz, 1H), 8.11 (d, *J* = 8.1 Hz, 1H), 7.66–7.56 (m, 2H), 6.84 (d, *J* = 9.1 Hz, 2H), 6.72 (d, *J* = 9.0 Hz, 2H), 5.72 (dd, *J* = 3.4, 11.5 Hz, 1H), 4.49 (s, 2H), 4.48–4.41 (m, 1H), 4.33 (d, *J* = 7.0 Hz, 1H), 3.37–3.30 (m, 2H, overlapping with MeOH), 2.78–2.70 (m, 1H), 2.49–2.37 (m, 1H), 2.36–2.18 (m, 1H), 2.15–1.99 (m, 3H), 1.71–1.52 (m, 3H), 0.96–0.81 (m, 12H); ^{13}C NMR (125 MHz, CD_3OD) δ 193.5, 181.8, 174.8, 173.2, 171.3, 165.5, 154.8, 153.4, 152.4, 138.4, 129.3, 128.5, 126.5, 123.7, 117.1, 117.0, 69.1, 59.2, 55.2, 53.3, 41.8, 41.5, 40.0, 33.8, 32.6, 28.8, 25.8, 23.2, 22.2, 19.8, 18.5; HRMS (ESI): *m*/*z* calcd for $C_{33}H_{42}N_5O_7S$ $[M+H]^+$ 652.2805, found 652.2839.

6.3.15. (*S*)-*N*-((*S*)-1-(Benzo[*d*]thiazol-2-yl)-1-oxo-3-((*S*)-2-oxopyrrolidin-3-yl)propan-2-yl)-2-((*S*)-2-(2-(4-(dimethylamino)phenoxy)acetamido)-3-methylbutanamido)-4-methylpentanamide (2o)

18% yield from **13c**; white powder; ^{1}H NMR (500 MHz, CD_3OD) δ 8.31 (d, *J* = 7.0 Hz, 1H), 8.21 (d, *J* = 8.0 Hz, 1H), 8.11 (d, *J* = 7.0 Hz, 1H), 7.67–7.57 (m, 2H), 7.25 (d, *J* = 8.7 Hz, 2H), 7.07 (d, *J* = 8.1 Hz, 2H), 5.73 (dd, *J* = 3.4, 11.6 Hz, 1H), 4.60 (s, 2H), 4.48–4.41 (m, 1H), 4.32 (d, *J* = 7.0 Hz, 1H), 3.42–3.32 (m, 2H), 2.78–2.69 (m, 1H), 2.50–2.42 (m, 1H), 2.24–2.17 (m, 1H), 2.14–2.03 (m, 3H), 1.70–1.52 (m, 3H), 0.99–0.82 (m, 12H); ^{13}C NMR (125 MHz, CD_3OD) δ 193.5, 181.8, 174.8, 173.3, 173.2, 170.7, 165.5, 154.8, 143.3, 138.4, 129.3, 128.5, 126.5, 123.8, 120.2, 117.3, 68.6, 59.4, 55.2, 53.4, 45.2, 41.8, 416, 40.0, 33.9, 32.5, 28.8, 25.8, 23.2, 22.2, 19.8, 18.5; HRMS (ESI): *m*/*z* calcd for $C_{35}H_{47}N_6O_6S$ $[M+H]^+$ 669.3278, found 669.3320.

6.3.16. (*S*)-*N*-((*S*)-1-(Benzo[*d*]thiazol-2-yl)-1-oxo-3-((*S*)-2-oxopyrrolidin-3-yl)propan-2-yl)-2-((*S*)-2-(2-(3-(dimethylamino)phenoxy)acetamido)-3-methylbutanamido)-4-methylpentanamide (2p)

37% yield from **13c**; light green solid; ^{1}H NMR (500 MHz, $CDCl_3$) δ 8.21 (br s, 1H, NH), 8.18–8.16 (d, *J* = 8.0 Hz, 1H), 7.99–7.97 (d, *J* = 8.0 Hz, 1H), 7.61–7.58 (m, 2H), 7.43–7.40 (m, 1H), 6.50–6.48 (d, *J* = 8.0 Hz, 1H), 6.44 (s, 1H), 6.38–6.36 (d, *J* = 8.0 Hz, 1H), 5.67–5.62 (m, 1H), 4.57–4.53 (m 1H), 4.52 (s, 2H), 4.34–4.31 (m, 1H), 3.40–3.32 (m, 2H), 3.01 (s, 6H), 2.60–2.53 (m, 2H), 2.17–2.02 (m, 3H), 2.00–1.89 (m, 1H), 1.72–1.52 (m, 3H), 0.96–0.89 (m, 12H); ^{13}C NMR (125 MHz, DMSO-d_6) δ 191.4, 178.2, 172.2, 171.3, 170.9, 164.1, 145.7, 141.1, 128.4, 128.3, 125.8, 57.4, 53.1, 50.8, 40.7, 39.4, 37.8, 36.6, 32.4, 31.2, 30.6, 27.5, 24.1, 22.9, 21.7, 19.2, 18.0; HRMS (ESI): *m*/*z* calcd for $C_{35}H_{48}N_6O_6S$ $[M+H]^+$ 679.3278, found 679.3287.

6.3.17. 4-(2-(((*S*)-1-(((*S*)-1-(((*S*)-1-(Benzo[*d*]thiazol-2-yl)-1-oxo-3-((*S*)-2-oxopyrrolidin-3-yl)propan-2-yl)amino)-4-methyl-1-oxopentan-2-yl)amino)-3-methyl-1-oxobutan-2-yl)amino)-2-oxoethoxy)benzoic acid (2q)

19% yield from **13c**; white powder; ^{1}H NMR (500 MHz, DMSO-d_6) δ 12.57 (br s, 1H), 8.70 (d, *J* = 7.4 Hz, 1H), 8.20 (d, *J* = 7.5 Hz, 1H), 8.16 (d, *J* = 7.2 Hz, 1H), 8.05 (d, *J* = 7.8 Hz, 1H), 7.89 (d, *J* = 8.9 Hz, 1H), 7.80 (d, *J* = 8.9 Hz, 2H), 7.63–7.55 (m, 2H), 6.93 (d, *J* = 8.9 Hz, 2H), 5.48–5.41 (m, 1H), 4.60 (dd, *J* = 14.8, 19.1 Hz, 1H), 4.29 (dd, *J* = 8.1, 14.7 Hz, 1H), 4.19 (dd, *J* = 6.6, 8.8 Hz, 1H), 3.14 (dd, *J* = 9.3, 8.9 Hz, 1H), 3.05 (dd, *J* = 7.4, 16.4 Hz, 1H), 2.42–2.37 (m, 1H, overlapping with DMSO), 2.22–2.14 (m, 1H), 2.10–2.02 (m, 1H), 1.94–1.84 (m, 1H), 1.82–1.71 (m, 2H), 1.50–1.41 (m, 1H), 1.38–1.28 (m, 2H), 0.75 (dd, *J* = 3.0, 6.6 Hz, 6H), 0.71 (d, *J* = 6.6 Hz, 6H); ^{13}C NMR (125 MHz, DMSO-d_6) δ 192.8, 178.0, 172.1, 170.3, 166.9, 166.8, 164.3, 161.3, 152.8, 136.3, 131.2, 128.1, 127.4, 125.2, 123.5, 123.1, 114.4, 66.6, 56.9, 53.2, 50.8, 40.7, 39.4, 37.8, 32.1, 30.9, 27.4, 24.0, 22.7, 21.7, 19.0, 17.9; HRMS (ESI): *m*/*z* calcd for $C_{34}H_{41}N_5O_8S$ $[M+H]^+$ 679.2676, found 679.2674.

6.3.18. (*S*)-*N*-((*S*)-1-(Benzo[*d*]thiazol-2-yl)-1-oxo-3-((*S*)-2-oxopyrrolidin-3-yl)propan-2-yl)-4-methyl-2-((*S*)-3-methyl-2-(2-(4-nitrophenoxy)acetamido)butanamido)pentanamide (2r)

12% yield from **13c**; white powder; ^{1}H NMR (500 MHz, CD_3OD) δ 8.89 (d, *J* = 7.9 Hz, 1H), 8.29 (d, *J* = 7.3 Hz, 1H), 8.26–8.20 (m, 3H), 8.12 (d, *J* = 7.6 Hz, 1H), 7.67–7.58 (m, 2H), 7.15 (d, *J* = 9.4 Hz, 2H), 5.77–5.70 (m, 1H), 4.75 (s, 2H), 4.44 (dd, *J* = 6.1, 14.4 Hz, 1H), 4.30 (d, *J* = 7.3 Hz, 1H), 3.41–3.32 (m, 2H, overlapping with MeOH), 2.77–2.69 (m, 1H), 2.49–2.42 (m, 1H), 2.25–2.18 (m, 1H), 2.13–2.02 (m, 3H), 1.68–1.53 (m, 3H), 0.99–0.83 (m, 12H); ^{13}C NMR (125 MHz, CD_3OD) δ 193.5, 181.8, 174.8, 173.2, 169.8, 154.8, 143.6, 138.4, 129.3, 128.5, 126.8, 126.5, 123.7, 116.2, 68.3, 59.7, 55.2, 53.3, 41.8, 41.5, 40.0, 33.9, 32.3, 28.8, 25.8, 23.2, 22.2, 19.8, 18.7; HRMS (ESI): *m*/*z* calcd for $C_{33}H_{40}N_6O_8S$ $[M+H]^+$ 680.2628, found 680.2627.

6.3.19. (*S*)-*N*-((*S*)-1-(Benzo[*d*]thiazol-2-yl)-1-oxo-3-((*S*)-2-oxopyrrolidin-3-yl)propan-2-yl)-4-methyl-2-((*S*)-3-methyl-2-(2-(pyridin-3-yloxy)acetamido)butanamido)pentanamide (2s)

33% yield from **13c**; white powder; ^{1}H NMR (500 MHz, CD_3OD) δ 8.54 (br s, 1H), 8.38 (d, *J* = 5.0 Hz, 1H), 8.31 (d, *J* = 7.3 Hz, 1H), 8.21

(d, J = 7.4 Hz, 1H), 8.11 (d, J = 7.0 Hz, 1H), 7.98 (dd, J = 2.8, 8.7 Hz, 1H), 7.79 (dd, J = 5.3, 8.7 Hz, 1H), 7.67–7.58 (m, 2H), 5.73 (dd, J = 3.5, 11.6 Hz, 1H), 4.85 (s, 2H), 4.45 (dd, J = 6.6, 14.2 Hz, 1H), 4.33–4.26 (m, 1H), 3.41–3.32 (m, 2H, overlapping with MeOH), 2.77–2.68 (m, 1H), 2.49–2.42 (m, 1H), 2.25–2.16 (m, 1H), 2.14–2.01 (m, 3H), 1.68–1.54 (m, 3H), 1.00–0.84 (m, 12H); ^{13}C NMR (125 MHz, CD_3OD) δ 193.5, 181.8, 174.9, 173.3, 169.4, 165.5, 157.6, 154.8, 138.5, 138.4, 134.3, 129.8, 129.3, 128.5, 128.0, 126.5, 123.8, 68.5, 59.9, 55.2, 53.3, 41.8, 41.5, 40.0, 33.9, 32.2, 28.8, 25.8, 23.2, 22.2, 19.8, 18.7; HRMS (ESI): m/z calcd for $C_{32}H_{41}N_6O_6S$ $[M+H]^+$ 637.2808, found 637.2809.

6.3.20. (*S*)-*N*-((*S*)-1-(Benzo[*d*]thiazol-2-yl)-1-oxo-3-((*S*)-2-oxopyrrolidin-3-yl)propan-2-yl)-4-methyl-2-((*S*)-3-methyl-2-(2-(phenylamino)acetamido)butanamido)pentanamide (2t)

17% yield from **13c**; slightly yellow powder; ^{1}H NMR (500 MHz, CD_3OD) δ 8.24 (d, J = 7.2 Hz, 1H), 8.20 (d, J = 7.8 Hz, 1H), 8.11 (d, J = 7.8 Hz, 1H), 7.67–7.57 (m, 2H), 7.19 (dd, J = 6.5, 8.4 Hz, 2H), 6.82 (t, J = 7.3 Hz, 1H), 6.75 (d, J = 7.9 Hz, 2H), 5.72 (dd, J = 3.4, 11.8 Hz, 1H), 4.41 (dd, J = 5.3, 14.0 Hz, 1H), 4.28 (d, J = 6.8 Hz, 1H), 3.85 (dd, J = 7.1, 10.9 Hz, 1H), 3.38–3.31 (m, 2H, overlapping with MeOH), 2.75–2.67 (m, 1H), 2.46–2.39 (m, 1H), 2.24–2.17 (m, 1H), 2.11–1.98 (m, 3H), 1.68–1.50 (m, 3H), 0.98–0.77 (m, 12H); ^{13}C NMR (125 MHz, CD_3OD) δ 193.5, 181.8, 174.8, 173.3, 172.7, 165.5, 154.8, 147.2, 138.4, 130.4, 129.3, 128.5, 126.7, 126.5, 123.7, 121.1, 115.6, 59.5, 55.1, 53.3, 41.8, 41.5, 39.9, 33.8, 32.5, 28.8, 25.8, 23.2, 22.2, 19.8, 18.3; HRMS (ESI): m/z calcd for $C_{33}H_{43}N_6O_5S$ $[M+H]^+$ 635.3016, found 635.3009.

6.3.21. (*S*)-*N*-((*S*)-1-(Benzo[*d*]thiazol-2-yl)-1-oxo-3-((*S*)-2-oxopyrrolidin-3-yl)propan-2-yl)-2-((*S*)-2-(2-(benzylamino)acetamido)-3-methylbutanamido)-4-methylpentanamide (2u)

22% yield from **13c**; yellow powder; ^{1}H NMR (500 MHz, CD_3OD) δ 8.21 (d, J = 7.2 Hz, 1H), 8.18 (d, J = 7.2 Hz, 1H), 8.09 (d, J = 7.8 Hz, 1H), 7.64–7.51 (m, 2H), 7.21 (dd, J = 6.5, 8.0 Hz, 2H), 6.83 (t, J = 7.3 Hz, 1H), 6.79 (d, J = 7.9 Hz, 2H), 5.73 (dd, J = 3.4, 11.8 Hz, 1H), 4.44 (dd, J = 5.1, 14.0 Hz, 1H), 4.31 (d, J = 6.4 Hz, 1H), 3.81 (s, 2H), 3.78 (dd, J = 7.1, 10.9 Hz, 1H), 3.40–3.34 (m, 2H, overlapping with MeOH), 2.75–2.70 (m, 1H), 2.46–2.40 (m, 1H), 2.24–2.20 (m, 1H), 2.10–2.00 (m, 3H), 1.70–1.50 (m, 3H), 1.00–0.77 (m, 12H); ^{13}C NMR (125 MHz, CD_3OD) δ 193.5, 181.8, 174.8, 173.3, 171.1, 165.5, 159.1, 154.8, 147.1, 138.4, 130.7, 129.3, 128.4, 125.3, 126.5, 123.7, 122.9, 121.1, 115.9, 68.1, 59.4, 55.2, 53.3, 41.8, 41.5, 40.0, 33.8, 32.5, 28.8, 25.8, 23.4, 22.2, 19.8, 18.3; HRMS (ESI): m/z calcd for $C_{34}H_{45}N_6O_5S$ $[M+H]^+$ 649.3172, found 649.3156.

6.4. Synthetic procedure for the preparation of 3a–d

Compounds **3a**–**d** was prepared from **13c** (2 mmol) with an appropriate dipeptidic **9** (1.1 equiv) using a procedure similar to that described for the preparation of **2a**. Compounds **3a**–**d** were purified by reverse phase HPLC.

6.4.1. Benzyl ((2*S*)-1-(((2*R*)-1-(((2*S*)-1-(benzo[*d*]thiazol-2-yl)-1-oxo-3-(2-oxopyrrolidin-3-yl)propan-2-yl)amino)-4-methyl-1-oxopentan-2-yl)amino)-3-methyl-1-oxobutan-2-yl)carbamate (3a)

22% yield from **13c**; White powder; ^{1}H NMR (500 MHz, DMSO-d_6) δ 8.21 (d, J = 8.4 Hz, 1H), 8.11 (d, J = 7.7 Hz, 1H), 7.66–7.57 (m, 2H), 7.37–7.26 (m, 5H), 5.72 (d, J = 8.3 Hz, 1H), 5.09 (s, 2H), 4.52–4.42 (m, 1H), 3.97–3.92 (m, 1H), 3.39–3.32 (m, 2H), 2.76–2.67 (m, 1H), 2.48–2.37 (m, 1H), 2.26–2.18 (m, 1H), 2.11–1.99 (m, 3H), 1.71–1.53 (m, 3H), 0.99–0.85 (m, 12H); HRMS (ESI): m/z calcd for $C_{33}H_{42}N_5O_6S$ $[M+H]^+$ 636.2856, found 636.2851.

6.4.2. Benzyl ((2*S*)-1-(((2*S*)-1-(((2*S*)-1-(benzo[*d*]thiazol-2-yl)-1-oxo-3-(2-oxopyrrolidin-3-yl)propan-2-yl)amino)-3-cyclohexyl-1-oxopropan-2-yl)amino)-3-methyl-1-oxobutan-2-yl)carbamate (3b)

26% yield from **13c**; white powder; ^{1}H NMR (500 MHz, DMSO-d_6) δ 8.74 (d, J = 8.0 Hz, 1H), 8.12 (d, J = 7.5 Hz, 1H), 8.10 (d, J = 3.2 Hz, 1H), 8.03 (d, J = 3.2 Hz, 1H), 7.94 (d, J = 8.2 Hz, 1H), 5.46–5.39 (m, 1H), 5.18 (s, 2H), 4.38 (dd, J = 8.4, 14.8 Hz, 1H), 3.88 (dd, J = 7.0, 8.6 Hz, 1H), 3.18 (dd, J = 8.7, 8.8 Hz, 1H), 3.11 (dd, J = 9.2, 16.3 Hz, 1H), 2.48–2.40 (m, 1H), 2.23–2.12 (m, 2H), 2.08–2.01 (m, 1H), 2.00–1.92 (m, 1H), 1.81–1.70 (m, 2H), 1.62–1.53 (m, 1H), 1.48–1.39 (m, 2H), 0.92–0.86 (m, 12H), 0.85–0.80 (m, 6H); HRMS (ESI): m/z calcd for $C_{36}H_{45}N_5O_6S$ $[M+H]^+$ 676.3169, found 676.3173.

6.4.3. Benzyl ((2*S*)-1-(((2*S*)-1-(((2*S*)-1-(benzo[*d*]thiazol-2-yl)-1-oxo-3-(2-oxopyrrolidin-3-yl)propan-2-yl)amino)-1-oxo-3-phenylpropan-2-yl)amino)-3-methyl-1-oxobutan-2-yl)carbamate (3c)

28% yield from **13c**; white powder; ^{1}H NMR (500 MHz, DMSO-d_6) δ 8.27 (d, J = 8.4 Hz, 1H), 8.16 (d, J = 7.7 Hz, 1H), 7.70–7.61 (m, 2H), 7.33–7.07 (m, 10H), 5.71 (d, J = 8.3 Hz, 1H), 5.10 (s, 2H), 4.53–4.42 (m, 1H), 3.99–3.93 (m, 1H), 3.39–3.32 (m, 4H), 2.80–2.71 (m, 1H), 2.60–2.55 (m, 1H), 2.30–2.22 (m, 1H), 2.11–1.99 (m, 3H), 1.00–0.89 (m, 6H); HRMS (ESI): m/z calcd for $C_{36}H_{40}N_5O_5S$ $[M+H]^+$ 670.2699, found 670.2685.

6.4.4. (4*S*)-5-(((2*S*)-1-(Benzo[*d*]thiazol-2-yl)-1-oxo-3-(2-oxopyrrolidin-3-yl)propan-2-yl)amino)-4-((*S*)-2-(((benzyloxy)carbonyl)amino)-3-methylbutanamido)-5-oxopentanoicacid (3d)

22% yield from **13c**; white powder; ^{1}H NMR (500 MHz, DMSO-d_6) δ 8.25 (d, J = 8.4 Hz, 1H), 8.23 (d, J = 7.7 Hz, 1H), 7.69–7.62 (m, 2H), 7.35–7.27 (m, 5H), 5.54 (d, J = 8.3 Hz, 1H), 5.04 (s, 1H), 4.45–4.39 (m, 1H), 3.37–3.31 (m, 2H), 3.15–3.14 (m, 2H), 2.27–2.12 (m, 2H), 1.98–1.84 (m, 3H), 1.65–1.40 (m, 3H), 1.24–1.02 (m, 2H), 0.86–0.82 (m, 6H); HRMS (ESI): m/z calcd for $C_{32}H_{37}N_5O_8S$ $[M+H]^+$ 652.2441, found 652.2432.

6.5. Synthetic procedure for the preparation of 4a–c

Compounds **4a**–**c** was prepared from **17** (2 mmol) with an appropriate dipeptidic **9** (1.1 equiv) using a procedure similar to that described for the preparation of **2a**. Compounds **4a**–**c** were purified by reverse phase HPLC.

6.5.1. Benzyl ((*S*)-1-(((*S*)-1-(((*S*)-3-(1*H*-imidazol-4-yl)-1-oxo-1-(thiazol-2-yl)propan-2-yl)amino)-4-methyl-1-oxopentan-2-yl)amino)-3-methyl-1-oxobutan-2-yl)carbamate (4a)

36% yield from **17**; colorless solid; ^{1}H NMR (300 MHz, DMSO-d_6) δ 8.81 (d, J = 9.60 Hz, 1H), 8.66 (d, J = 13.6 Hz, 1H), 8.27 (br s, 1H), 8.16–8.13 (m, 1H), 7.81 (t, J = 19.6 Hz, 1H), 7.31–7.24 (br s, 2H), 6.98–6.91 (m, 3H), 4.56 (s, 1H), 431–4.18 (m, 2H), 3.25 (br s, 1H), 1.93–191 (m, 1H), 1.36–1.24 (m, 3H), 0.84–0.70 (m, 12H); HRMS (ESI): m/z calcd for $C_{28}H_{36}N_6O_5S$ $[M+H]^+$ 569.2535, found 569.2546.

6.5.2. (*S*)-*N*-((*S*)-3-(1*H*-imidazol-4-yl)-1-oxo-1-(thiazol-2-yl)propan-2-yl)-4-methyl-2-((*S*)-3-methyl-2-(2-phenoxyacetamido)butanamido)pentanamide (4b)

43% yield from **17**; colorless solid; ^{1}H NMR (300 MHz, DMSO-d_6) δ 8.89 (d, J = 4.65 Hz, 1H), 8.70–8.69 (m, 1H), 8.28 (br s, 1H),

8.15 (t, J = 6.27 Hz, 1H), 7.37–7.33 (m, 2H), 7.20 (t, J = 13.7 Hz, 2H), 7.08 (d, J = 8.1 Hz, 2H), 4.36–4.34 (m, 1H), 3.92–3.86 (m, 1H), 3.26 (br s, 1H), 1.98–1.96 (m, 1H), 1.37–1.23 (m, 3H), 0.84–0.81 (m, 12H); HRMS (ESI): m/z calcd for $C_{28}H_{36}N_6O_5S$ $[M+H]^+$ 569.2527, found 569.2546.

6.5.3. Phenyl ((*S*)-1-(((*S*)-1-(((*S*)-3-(1*H*-imidazol-4-yl)-1-oxo-1-(thiazol-2-yl)propan-2-yl)amino)-4-methyl-1-oxopentan-2-yl)amino)-3-methyl-1-oxobutan-2-yl)carbamate (4c)

38% yield from **17**; colorless solid; ^{1}H NMR (300 MHz, $CDCl_3$) δ 8.57 (t, J = 13.6 Hz, 1H), 7.20 (t, J = 14.7 Hz, 1H), 7.10 (d, J = 7.73 Hz, 2H), 4.59 (br s, 1H), 4.11 (br s, 1H), 1.64 (br s, 2H), 1.26 (t, J = 4.1 Hz, 2H), 0.9–0.93 (m, 9H); HRMS (ESI): m/z calcd for $C_{27}H_{34}N_6O_5S$ $[M+H]^+$ 569.2527, found 569.2546.

6.6. Synthetic procedure for the preparation of 5a–i

Compound **5a–i** was prepared from **13d–i** (2 mmol) with an appropriate dipeptidic **9** (1.1 equiv) using a procedure similar to that described for the preparation of **2a**. Compounds **5a–i** were purified by reverse phase HPLC.

6.6.1. Benzyl ((2*S*)-3-methyl-1-(((2*S*)-4-methyl-1-oxo-1-(((2*S*)-1-oxo-3-(2-oxopyrrolidin-3-yl)-1-(5-phenylthiazol-2-yl)propan-2-yl)amino)pentan-2-yl)amino)-1-oxobutan-2-yl)carbamate (5a)

33% yield from **13e**; colorless solid; ^{1}H NMR (400 MHz, $CDCl_3$) δ 8.15 (s, 1H), 7.62–7.61 (m, 2H), 7.47–7.40 (m, 2H), 7.37–7.24 (m, 5H), 5.41–5.33 (m, 1H), 5.15 (s, 1H), 4.58–4.52 (m, 2H), 4.07–4.03 (m, 1H), 3.36–3.29 (m, 2H), 2.61–2.55 (m, 2H), 2.16–1.96 (m, 3H), 1.81–1.70 (m, 2H), 1.62–1.53 (m, 1H), 1.48–1.39 (m, 2H), 0.99–0.88 (m, 12H); ^{13}C NMR (400 MHz, DMSO-d_6) δ 191.5, 177.9, 172.2, 170.8, 162.9, 156.1, 146.4, 141.3, 137.1, 129.8, 129.7, 128.2, 127.6, 127.1, 65.3, 60.3, 53.6, 52.7, 60.7, 32.3, 30.3, 30.2, 28.1, 27.2, 24.0, 22.8, 21.7, 19.1, 18.0; HRMS (ESI): m/z calcd for $C_{35}H_{44}N_5O_6S$ $[M+H]^+$ 662.3012, found 662.3018.

6.6.2. (2*S*)-2-((*S*)-2-(2-(4-Methoxyphenoxy)acetamido)-3-methylbutanamido)-4-methyl-*N*-((2*S*)-1-oxo-3-(2-oxopyrrolidin-3-yl)-1-(5-phenylthiazol-2-yl)propan-2-yl)pentanamide (5b)

45% yield from **13e**; colorless solid; ^{1}H NMR (400 MHz, $CDCl_3$) δ 8.16 (s, 1H), 7.64–7.61 (d, J = 8.4 Hz, 2H), 7.48–7.40 (m, 3H), 6.92–6.83 (m, 4H), 5.68–5.62 (m, 1H), 4.55–4.50 (m 1H), 4.48 (s, 2H), 4.34–4.30 (m, 1H), 3.77 (s, 3H), 3.40–3.29 (m, 2H), 2.61–2.44 (m, 2H), 2.19–2.02 (m, 3H), 1.91–1.85 (m, 1H), 1.71–1.53 (m, 3H), 0.96–0.88 (m, 12H); ^{13}C NMR (400 MHz, DMSO-d_6) δ 191.0, 185.7, 178.7, 174.3, 172.3, 168.2, 164.0, 162.4, 156.8, 153.8, 151.4, 146.6, 140.9, 139.2, 129.8, 129.4, 127.0, 122.2, 115.5, 114.4, 67.2, 57.4, 55.3, 52.7, 51.0, 48.9, 47.1, 32.7, 30.4, 27.1, 24.0, 22.5, 21.4, 21.2, 18.8, 17.5; HRMS (ESI): m/z calcd for $C_{36}H_{47}N_5O_7S$ $[M+H]^+$ 692.3118, found 692.3145.

6.6.3. (2*S*)-2-((*S*)-2-(2-(4-Methoxyphenoxy)acetamido)-3-methylbutanamido)-4-methyl-*N*-((2*S*)-1-oxo-3-(2-oxopyrrolidin-3-yl)-1-(5-(p-tolyl)thiazol-2-yl)propan-2-yl)pentanamide (5c)

47% yield from **13f**; colorless solid; ^{1}H NMR (400 MHz, $CDCl_3$) δ 8.12 (s, 1H), 7.51–7.49 (d, J = 8.4 Hz, 2H), 7.26–7.24 (d, J = 8.0 Hz, 2H), 6.89–6.83 (m, 4H), 5.64–5.59 (m, 1H), 4.57–4.52 (m, 1H), 4.48 (s, 2H), 3.77 (s, 3H), 3.38–3.29 (m, 2H), 2.59–2.53 (m, 2H), 2.40 (s, 3H), 2.29–2.01 (m, 4H), 1.75–1.56 (m, 3H), 0.96–0.87 (m, 12H); ^{13}C NMR (400 MHz, DMSO-d_6) δ 191.4, 177.7, 176.3, 172.1, 170.3, 167.7, 162.3, 153.7, 151.5, 146.6, 140.8, 139.7, 129.9, 127.0, 115.5, 114.54, 67.3, 57.1, 55.3, 53.6, 52.6, 50.8, 38.87, 32.4, 30.6, 28.1, 27.3, 24.0, 22.8, 21.7, 20.8, 19.1, 19.0, 17.8; HRMS (ESI): m/z calcd for $C_{37}H_{49}N_5O_7S$ $[M+H]^+$ 706.3274, found 706.3275.

6.6.4. (2*S*)-2-((*S*)-2-(2-(4-Methoxyphenoxy)acetamido)-3-methylbutanamido)-*N*-((2*S*)-1-(5-(4-methoxyphenyl)thiazol-2-yl)-1-oxo-3-(2-oxopyrrolidin-3-yl)propan-2-yl)-4-methylpentanamide (5d)

40% yield from **13g**; yellow solid; ^{1}H NMR (400 MHz, $CDCl_3$) δ 8.09 (s, 1H), 7.58–7.56 (d, J = 8.0 Hz, 2H), 6.99–6.97 (d, J = 8.4 Hz, 2H), 6.92–6.84 (m, 4H), 5.66–5.62 (m, 1H), 4.51–4.50 (m, 1H), 4.48 (s, 2H), 4.33–4.30 (m, 1H), 3.89 (s, 3H), 3.77 (s, 3H), 3.38–3.31 (m, 2H), 2.60–2.53 (m, 2H), 2.30–2.01 (m, 4H), 1.77–1.56 (m, 3H), 0.96–0.87 (m, 12H); ^{13}C NMR (400 MHz, DMSO-d_6) δ 191.0, 178.0, 172.1, 170.3, 167.7, 161.4, 160.5, 153.7, 151.6, 146.7, 140.2, 128.7, 122.2, 115.2, 114.8, 67.3, 56.8, 55.3, 52.6, 50.8, 32.4, 30.9, 30.6, 28.1, 27.2, 24.1, 24.0, 22.8, 21.7, 21.5, 19.1, 17.8; HRMS (ESI): m/z calcd for $C_{37}H_{49}N_5O_8S$ $[M+H]^+$ 722.3224, found 722.3237.

6.6.5. (2*S*)-*N*-((2*S*)-1-(5-(4-Chlorophenyl)thiazol-2-yl)-1-oxo-3-(2-oxopyrrolidin-3-yl)propan-2-yl)-2-((S)-2-(2-(4-methoxyphenoxy)acetamido)-3-methylbutanamido)-4-methylpentanamide (5e)

47% yield from **13h**; yellow solid; ^{1}H NMR (400 MHz, $CDCl_3$) δ 8.06 (s, 1H), 7.48–7.46 (d, J = 8.0 Hz, 2H), 7.34–7.32 (d, J = 8.4 Hz, 2H), 6.82–6.73 (m, 4H), 5.57–5.52 (m, 1H), 4.41–4.40 (m, 1H), 4.38 (s, 2H), 4.22–4.17 (m, 1H), 3.67 (s, 3H), 3.30–3.19 (m, 2H), 2.53–2.38 (m, 2H), 2.04–1.90 (m, 4H), 1.57–1.42 (m, 3H), 0.96–0.87 (m, 12H); ^{13}C NMR (125 MHz, DMSO-d_6) δ 191.4, 178.2, 172.1, 170.4, 167.9, 163.1, 153.7, 151.5, 145.0, 141.7, 134.4, 129.4, 128.8, 128.6, 115.5, 114.5, 67.2, 57.2, 55.2, 53.6, 52.7, 50.7, 32.2, 30.8, 30.5, 27.2, 24.0, 22.7, 21.6, 21.5, 19.0, 18.9, 17.7; HRMS (ESI): m/z calcd for $C_{36}H_{46}N_5O_7SCl$ $[M+H]^+$ 726.2728, found 726.2723.

6.6.6. (2*S*)-2-((*S*)-2-(2-(4-Methoxyphenoxy)acetamido)-3-methylbutanamido)-4-methyl-*N*-((2*S*)-1-(5-(naphthalen-2-yl)thiazol-2-yl)-1-oxo-3-(2-oxopyrrolidin-3-yl)propan-2-yl)pentanamide (5f)

42% yield from **13i**; yellow solid; ^{1}H NMR (400 MHz, $CDCl_3$) δ 8.29–8.28 (d, J = 4.6 Hz, 1H), 8.10 (s, 1H), 7.91–7.87 (m, 3H), 7.71–7.69 (t, J = 8.4 Hz, 1H), 7.60–7.53 (m, 1H), 7.36–7.33 (m, 1H), 6.92–6.83 (m, 4H), 7.70–5.67 (m, 1H), 4.55–4.51 (m, 1H), 4.48 (s, 2H), 4.37–4.33 (m, 1H), 3.76 (s, 3H), 3.39–3.29 (m, 2H), 2.64–2.2.50 (m, 2H), 2.39–2.33 (m, 1H), 2.19–2.04 (m, 2H), 1.91–1.86 (m, 1H), 1.71–1.55 (m, 3H), 0.96–0.89 (m, 12H); ^{13}C NMR (400 MHz, DMSO-d_6) δ 191.0, 178.2, 172.2, 170.4, 167.9, 162.6, 153.8, 151.5, 146.6, 141.5, 133.1, 129.0, 128.2, 127.6, 127.2, 127.1, 124.3, 115.4, 114.5, 67.2, 56.9, 55.2, 52.7, 50.9, 48.5, 32.3, 30.5, 27.2, 24.0, 22.7, 21.6, 19.0, 17.7; HRMS (ESI): m/z calcd for $C_{40}H_4N_5O_5SNa$ $[M+Na]^+$ 764.3094, found 764.3095.

6.6.7. (2*S*)-2-((*S*)-2-(2-(4-Methoxyphenoxy)acetamido)-3-methylbutanamido)-*N*-((2*S*)-1-(5-(2-methoxyphenyl)thiazol-2-yl)-1-oxo-3-(2-oxopyrrolidin-3-yl)propan-2-yl)-4-methylpentanamide (5g)

39% yield from **13j**; colorless solid; ^{1}H NMR (400 MHz, $CDCl_3$) δ 8.14 (s, 1H), 8.08 (br s, 1H, NH), 7.38–7.34 (t, J = 8.0 Hz, 1H), 7.21–7.19 (d, J = 7.2 Hz, 1H), 7.13–7.09 (m, 1H), 6.99–6.87 (m, 2H), 6.83–6.80 (m, 2H), 5.70–5.56 (m, 1H), 4.62–4.52 (m, 1H), 4.48 (s, 2H), 4.31–4.30 (m, 1H), 3.86 (s, 3H), 3.77 (s, 3H), 3.41–3.37 (m, 2H), 2.63–2.50 (m, 2H), 2.33–2.21 (m, 1H), 2.20–2.09 (m, 2H), 1.91–1.86 (m, 2H), 1.71–1.55 (m, 3H), 0.95–0.86 (m, 12H); ^{13}C NMR (400 MHz, DMSO-d_6) δ 191.1, 177.9, 171.3, 167.6, 162.6, 159.6, 153.7, 151.6, 146.2, 141.6, 131.0, 130.6, 127.1, 119.6, 115.5,

114.5, 112.4, 67.3, 56.8, 60.8, 52.7, 50.8, 32.4, 27.2, 24.0, 22.8, 21.6, 19.1, 17.8; HRMS (ESI): *m*/*z* calcd for $C_{37}H_{47}N_5O_8SNa$ $[M+Na]^+$ 744.3043, found 744.3051.

6.6.8. (2*S*)-2-((*S*)-2-(2-(3-(Dimethylamino)phenoxy)acetamido)-3-methylbutanamido)-4-methyl-*N*-((2*S*)-1-oxo-3-(2-oxopyrrolidin-3-yl)-1-(5-phenylthiazol-2-yl)propan-2-yl)pentanamide (5h)

36% yield from **13e**; light green solid; ^{1}H NMR (400 MHz, $CDCl_3$) δ 8.16 (s, 1H), 8.10 (br s, 1H, NH), 7.61–7.58 (m, 2H), 7.44–7.41 (m, 3H), 7.22–7.16 (m, 1H), 6.52–6.50 (d, J = 8.0 Hz, 1H), 6.45 (s, 1H), 6.38–6.36 (d, J = 8.0 Hz, 1H), 5.68–5.63 (m, 1H), 4.58–4.53 (m 1H), 4.54 (s, 2H), 4.35–4.31 (m, 1H), 3.37–3.31 (m, 2H), 2.97 (s, 6H), 2.61–2.57 (m, 2H), 2.18–2.03 (m, 3H), 1.99–1.89 (m, 1H), 1.71–1.54 (m, 3H), 0.96–0.89 (m, 12H); ^{13}C NMR (400 MHz, DMSO-d_6) δ 191.1, 177.9, 170.3, 167.5, 162.6, 158.6, 146.4, 141.3, 129.4, 127.1, 102.6, 66.5, 56.7, 53.8, 32.4, 27.1, 24.0, 22.8, 21.7, 19.0 17.8; HRMS (ESI): *m*/*z* calcd for $C_{37}H_{50}N_6O_6S$ $[M+H]^+$ 705.3434, found 705.3429.

6.6.9. (2*S*)-2-((*S*)-2-(2-(3-(Dimethylamino)phenoxy)acetamido)-3-methylbutanamido)-4-methyl-*N*-((2*S*)-1-(5-methylthiazol-2-yl)-1-oxo-3-(2-oxopyrrolidin-3-yl)propan-2-yl)pentanamide (5i)

35% yield from **13d**; light green solid; ^{1}H NMR (400 MHz, $CDCl_3$) δ 8.10 (br s, 1H, NH), 7.66 (s, 1H), 7.43–7.23 (t, J = 8.4 Hz, 1H), 6.88–6.85 (m, 2H), 6.70 (s, 1H), 5.60–5.58 (m, 1H), 4.58–4.53 (m, 1H), 4.50 (s, 2H), 4.37–4.33 (m, 1H), 3.36–3.27 (m, 2H), 3.08 (s, 6H), 2.61–2.44 (m, 5H), 2.15–2.01 (m, 3H), 1.91–1.85 (m, 1H), 1.64–1.53 (m, 3H), 0.94–0.86 (m, 12H); ^{13}C NMR (400 MHz, DMSO-d_6) δ 191.4, 177.9, 172.0, 170.3, 167.6, 162.7, 162.4, 158.6, 150.9, 143.6, 129.7, 106.6, 103.4, 99.9, 66.6, 57.0, 53.5, 50.8, 32.5, 31.0, 28.1, 27.2, 24.0, 22.8, 21.7, 21.6, 19.1, 19.0, 17.8; HRMS (ESI): *m*/*z* calcd for $C_{32}H_{48}N_6O_6S$ $[M+H]^+$ 643.3278, found 643.3259.

6.7. Biological evaluation

6.7.1. Estimation of IC_{50} value

IC_{50} value of each inhibitor was assessed from the apparent decrease of a substrate (H-TSAVLQSGFRK-NH_2) by the digestion with R188I SARS 3CL protease as described previously.[30,29] Briefly, the substrate (111 μM) in a reaction solution (25 μL of 20 mM Tris–HCl buffer pH 7.5 containing 7 mM DTT) was incubated with the R188I SARS protease (56 nM) at 37 °C for 60 min in the presence of various inhibitor concentrations. The cleavage reaction was monitored by analytical HPLC [Cosmosil 5C18 column (4.6 × 150 mm), a linear gradient of CH_3CN (10–20%) in an aq 0.1% TFA over 30 min], and the cleavage rates were calculated from the decease of the substrate peak area. Each IC_{50} value was obtained from the sigmoidal dose–response curve. Each experiment was repeated 3 times and the results were averaged.

6.7.2. Estimation of K_i value

Inhibition constants, K_i, were assessed by determining the apparent kinetic parameters at a constant substrate concentration (10 μM) and different inhibitor concentrations (0–200 μM) at 25 °C. The initial rate measurements were determined as previously described using a fluorescence-based peptide cleavage assay with a commercially available fluorogenic substrate, Dabcyl-KTSAVLQSGFRKME-Edans (Genesis Biotech).[24,31] The change in fluorescence intensity was monitored in a Cary Eclipse fluorescence spectrophotometer (Varian) with 355 and 538 nm excitation and emission wavelengths, respectively. Substrate was dissolved in deionized water, and inhibitors were dissolved in DMSO. The experiments were performed in a buffer containing10 mM sodium phosphate, 10 mM sodium chloride, 1 mM EDTA, 1 mM TCEP and 2% DMSO (pH 7.4). While varying inhibitor concentrations (0–200 μM), the reaction was initiated by adding protease (final concentration 100 nM) to a solution of substrate at final concentration of 10 μM to a total volume of 120 μL in a microcuvette. The data from these assays were analyzed by using the non-linear regression analysis software Origin 7.

Acknowledgments

This research was supported by Grants from the Ministry of Education, Culture, Sports, Science and Technology (MEXT) of Japan, including a Grant-in-aid for Young scientist (*Tokubetsu Kenkyuin Shorei-hi*) 23·01104 and a Grant-in-aid for Scientific Research 23659059.

References and notes

1. Ksiazek, T. G.; Erdman, D.; Goldsmith, C. S.; Zaki, S. R.; Peret, T.; Emery, S.; Tong, S.; Urbani, C.; Comer, J. A.; Lim, W.; Rollin, P. E.; Dowell, S. F.; Ling, A. E.; Humphrey, C. D.; Shieh, W. J.; Guarner, J.; Paddock, C. D.; Roca, P.; Fields, B.; DeRisi, J.; Yang, J. Y.; Cox, N.; Hughes, J. M.; LeDuc, J. W.; Bellini, W. J.; Anderson, L. J. *N. Engl. J. Med.* **2003**, *348*, 1953.
2. Drosten, C.; Gunther, S.; Preiser, W.; van der Werf, S.; Brodt, H. R.; Becker, S.; Rabenau, H.; Panning, M.; Kolesnikova, L.; Fouchier, R. A. M.; Berger, A.; Burguiere, A. M.; Cinatl, J.; Eickmann, M.; Escriou, N.; Grywna, K.; Kramme, S.; Manuguerra, J.-C.; Muller, S.; Rickerts, V.; Sturmer, M.; Vieth, S.; Klenk, H. D.; Osterhaus, A. D. M. E.; Schmitz, H.; Doerr, H. W. *N. Engl. J. Med.* **2003**, *348*, 1967.
3. Peiris, J. S.; Lai, S. T.; Poon, L. L.; Guan, Y.; Yam, L. Y.; Lim, W.; Nicholls, J.; Yee, W. K.; Yan, W. W.; Cheung, M. T.; Cheng, V. C.; Chan, K. H.; Tsang, D. N.; Yung, R. W.; Ng, T. K.; Yuen, K. Y. *Lancet* **2003**, *361*, 1319. and references therein.
4. World Health Organization, Communicable Disease Surveillance & Response, website: http://www.who.int/csr/sars/archive/2003_05_07a/en and http://www.who.int/csr/sars/country/en/Country2003_08_15.pdf. Summary table of SARS cases by country (1 November 2002 to 7 August 2003).
5. Lee, N.; Hui, D.; Wu, A.; Chan, P.; Cameron, P.; Joynt, G. M.; Ahuja, A.; Yung, M. Y.; Leung, C. B.; To, K. F.; Lui, S. F.; Szeto, C. C.; Chung, S.; Sung, J. J. Y. *N. Engl. J. Med.* **2003**, *348*, 1986.
6. Anand, K.; Ziebuhr, J.; Wadhwani, P.; Mesturs, J. R.; Hilgenfeld, R. *Science* **2003**, *300*, 1763.
7. Rota, P. A.; Oberste, M. S.; Nix, W. A.; Campagnoli, R.; Icenogle, J. P.; Penaranda, S.; Bankamp, B.; Maher, K.; Chen, M. H.; Tong, S.; Tamin, A.; Lowe, L.; Frace, M.; DeRisi, J. L.; Chen, Q.; Wang, D.; Erdman, D. D.; Peret, T. C. T.; Burns, C.; Ksiazek, T. G.; Rollin, P. E.; Sanchez, A.; Liffick, S.; Holloway, B.; Limor, J.; McCaustland, K.; Olsen-Rasmussen, M.; Fouchier, R.; Gunther, S.; Osterhaus, A. D. H. E.; Drosten, C.; Pallansch, M. A.; Anderson, L. J.; Bellini, W. J. *Science* **2003**, *300*, 1394.
8. Thiel, V.; Ivanov, K. A.; Putics, A. A.; Hertzig, T.; Schelle, B.; Bayer, S.; Weiabrich, B.; Snijder, E. J.; Rabenau, H.; Doerr, H. W.; Ziebuhr, J. *J. Gen. Virol.* **2003**, *84*, 2305.
9. Yang, H.; Yang, M.; Ding, Y.; Liu, Y.; Lou, Z.; Zhou, Z.; Sun, L.; Mo, L.; Ye, S.; Pang, H.; Gao, G. F.; Anand, K.; Bartlam, M.; Hilgenfeld, R.; Rao, Z. *Proc. Natl. Acad. Sci. U.S.A.* **2003**, *100*, 13190.
10. Chou, K.; Wei, D.; Zhong, W. *Biochem. Biophys. Res. Commun.* **2003**, *308*, 148.
11. Wu, C. Y.; Jan, J. T.; Ma, S. H.; Kuo, C. J.; Juan, H. F.; Cheng, Y. S. E.; Hsu, H. H.; Huang, H. C.; Wu, D.; Ashraf, B.; Liang, F. S.; Liu, R. S.; Fang, J. M.; Chen, S. T.; Liang, P. H.; Wong, C. H. *Proc. Natl. Acad. Sci. U.S.A.* **2004**, *101*, 10012.
12. Kao, R. Y.; Tsui, W. H. W.; Lee, T. S. W.; Tanner, J. A.; Watt, R. M.; Huang, J. D.; Hu, L. H.; Chen, G. H.; Chen, Z. W.; Zhang, L. Q.; He, T.; Chan, K. H.; Tse, H.; To, A. P. C.; Ng, L. W. Y.; Wong, B. C. W.; Tsoi, H. W.; Yang, D.; Ho, D. D.; Yuen, K. Y. *Chem. Biol.* **2004**, *11*, 1293.
13. Bacha, U.; Barrila, J.; Velazquez-Campoy, A.; Leavitt, S. A.; Freire, E. *Biochemistry* **2004**, *43*, 4906.
14. Jain, R. P.; Pettersson, H. I.; Zhang, J. M.; Aull, K. D.; Fortin, P. D.; Huitema, C.; Eltis, L. D.; Parrish, J. C.; James, M. N. G.; Wishart, D. S.; Vederas, J. C. *J. Med. Chem.* **2004**, *47*, 6113.
15. Chen, L. R.; Wang, Y. C.; Lin, Y. W.; Chou, S. Y.; Chen, S. F.; Liu, L. T.; Wu, Y. T.; Chih-Jung, K. B.; Chen, T. S. S.; Juang, S. H. *Bioorg. Med. Chem. Lett.* **2005**, *15*, 3058.
16. Blanchard, J. E.; Elowe, N. H.; Huitema, C.; Fortin, P. D.; Cechetto, J. D.; Eltis, L. D.; Brown, E. D. *Chem. Biol.* **2004**, *11*, 1445.
17. Hsu, J. T. A.; Kuo, C. J.; Hsieh, H. P.; Wang, Y. C.; Huang, K. K.; Lin, C. P. C.; Huang, P. F.; Chen, X.; Liang, P. H. *FEBS Lett.* **2004**, *574*, 116.
18. Chen, L. L.; Gui, C. S.; Luo, X. M.; Yang, Q. G.; Gunther, S.; Scandella, E.; Drosten, C.; Bai, D.; He, X. C.; Ludewig, B.; Chen, J.; Luo, H. B.; Yang, Y. M.; Yang, Y. F.; Zou, J. P.; Thiel, V.; Chen, K.; Shen, J. H.; Xu, S.; Jiang, H. L. *J. Virol.* **2005**, *79*, 7095.
19. Liu, Z.; Huang, C.; Fan, K.; Wei, P.; Chen, H.; Liu, S.; Pei, J.; Shi, L.; Li, B.; Yang, K.; Liu, Y.; Lai, L. *J. Chem. Inf. Model.* **2005**, *45*, 10.
20. Wu, C. Y.; King, K. Y.; Kuo, C. J.; Fang, J. M.; Wu, Y. T.; Ho, M. Y.; Liao, C. L.; Shie, J. J.; Liang, P. H.; Wong, C. H. *Chem. Biol.* **2006**, *13*, 4469.

21. Ghosh, A. K.; Xi, K.; Grum-Tokars, V.; Xu, X.; Ratia, K.; Fu, W.; Houser, K. V.; Baker, S. C.; Johnson, M. E.; Mesecar, A. D. *Bioorg. Med. Chem. Lett.* **2007**, *17*, 5876.
22. Shie, J. J.; Fang, J. M.; Kuo, T. H.; Kuo, C. J.; Liang, P. H.; Huang, H. J.; Yang, W. B.; Lin, C. H.; Chen, J. L.; Wu, Y. T.; Wong, C. H. *J. Med. Chem.* **2005**, *48*, 4469.
23. Sydnes, M. O.; Hayashi, Y.; Sharma, V. K.; Hamada, T.; Bacha, U.; Barrila, J.; Freire, E.; Kiso, Y. *Tetrahedron* **2006**, *62*, 8601.
24. Bacha, U.; Barrila, J.; Gabelli, B.; Kiso, Y.; Amzel, L. M.; Freire, E. *Chem. Biol. Drug Des.* **2008**, *72*, 34.
25. Regnier, T.; Sharma, D.; Hidaka, K.; Bacha, U.; Freire, E.; Hayashi, Y.; Kiso, Y. *Bioorg. Med. Chem. Lett.* **2009**, *19*, 2722.
26. Tian, Q.; Nayyar, N. K.; Babu, S.; Chen, L.; Tao, J.; Lee, S.; Tibbetts, A.; Moran, T.; Liou, J.; Guo, M.; Kennedy, T. P. *Tetrahedron Lett.* **2001**, *42*, 6807.
27. Webber, S. E.; Okano, K.; Little, T. L.; Reich, S. H.; Xin, Y.; Fuhrman, S. A.; Matthews, D. A.; Love, R. A.; Hendrickson, T. F.; Patick, A. K.; Meador, J. W., III; Ferre, R. A.; Brown, E. L.; Ford, C. E.; Binford, S. L.; Worland, S. T. *J. Med. Chem.* **1998**, *41*, 2786.
28. Akaji, K.; Konno, H.; Onozuka, M.; Makino, A.; Saito, H.; Nosaka, K. *Bioorg. Med. Chem.* **2008**, *16*, 9400.
29. Akaji, K.; Konno, H.; Mitsui, H.; Teruya, K.; Shimamoto, Y.; Hattori, Y.; Ozaki, T.; Kusunoki, M.; Sanjoh, A. *J. Med. Chem.* **2011**, *54*, 7962.
30. Barrila, J.; Bacha, U.; Freire, E. *Biochemistry* **2006**, *45*, 14908.
31. Yang, H.; Xie, W.; Xue, X.; Yang, K.; Ma, J.; Liang, W.; Zhao, Q.; Zhou, Z.; Pei, D.; Ziebuhr, J.; Hilgenfeld, R.; Yuen, K. Y.; Wong, L.; Gao, G.; Chen, S.; Chen, Z.; Ma, D.; Bartlam, M.; Rao, Z. *PLoS Biol.* **2005**, *3*, 1742.
32. The values quoted as minimized docking energies are non-bonded energy between the protease and inhibitors, which was calculated by Molecular Operating Environment (MOE) system.